The Magnetic Sail

Final Report to the NASA Institute of Advanced Concepts (NIAC)

January 7, 2000

Principal Investigator: **Robert Zubrin**

Co-Investigator: **Andrew Martin**

Pioneer Astronautics
445 Union Blvd. Suite #125
Lakewood, CO 80228
303-980-0890

Table of Contents:

Introduction:

The magnetic sail [1,2,3,4,5,6,7] or magsail, is a device which can be used to accelerate or decelerate a spacecraft by using a magnetic field to accelerate/deflect the plasma naturally found in the solar wind and interstellar medium. Its principle of operation is as follows:

A loop of superconducting cable perhaps tens of kilometers in diameter is stored on a drum attached to a payload spacecraft. When the time comes for operation, the cable is played out and a current is initiated in the loop. This current once initiated, will be maintained indefinitely in the superconductor without further power. The magnetic field created by the current will impart a hoop stress to the loop aiding the deployment and eventually forcing it to a rigid circular shape. The loop operates at low field strengths, typically 0.0001 Tesla, so little structural strengthening is required. The loop can be positioned with its dipole axis at any angle with respect to the plasma wind, with the two extreme cases examined for analytical purposes being the axial configuration, in which the dipole axis is parallel to the wind, and the normal configuration, in which the dipole axis is perpendicular to the wind. A magsail with payload is depicted in Fig. 1.

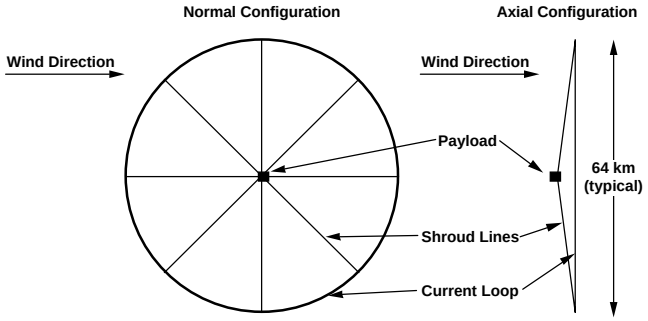

Figure 1. Magsail deployed with payload

In operation, charged particles entering the field are deflected according to the B-field they experience, thus imparting momentum to the loop. If a net plasma wind, such as the solar wind, exists relative to the spacecraft, the magsail loop will always create drag, and thus accelerate the spacecraft in the direction of the relative wind. The solar wind in the vicinity of the Earth is a flux of several million protons and electrons per cubic meter at a velocity of 400 to 600 km/s. This can be used to accelerate a spacecraft radially away from the sun and the maximum speed available would be that of the solar wind itself. While inadequate for interstellar missions, these velocities are certainly more than adequate for interplanetary missions.

However if the magsail spacecraft has somehow been accelerated to a relevant interstellar velocity, for example by a fusion rocket or a laser-pushed lightsail, the magsail can be used to create drag against the static interstellar medium, and thus act as an effective braking device. The ability to slow spacecraft from relativistic to

interplanetary velocities without the use of rocket propellant results in a dramatic lowering of both rocket mass ratio and the mission time.

If the magsail is utilized in a non-axial configuration, symmetry is destroyed and it becomes possible for the magsail to generate a force perpendicular to the wind, i.e. lift. Lift can be used to alter the magsail spacecraft's angular momentum about the sun, thus greatly increasing the repertoire of possible maneuvers. In addition, lift can be used to provide steering ability to a decelerating relativistic interstellar spacecraft.

The magsail as currently conceived depends on operating the superconducting loop at high current densities at ambient temperatures. In interstellar space, ambient is 2.7 degrees K, where current low temperature superconductors NbTi and Nb_3Sn have critical currents (depending upon temperature and local magnetic field) of approximately $1.0x10^{10}$ and $2.0x10^{10}$ Amps/m^2 respectively. In interplanetary space, where ambient temperatures are above the critical temperatures of low temperature superconductors, these materials would require expensive and heavy refrigeration systems However the new high temperature superconductors such as $YBa_2Cu_3O_7$ have demonstrated comparable critical currents in microscopic samples at temperatures of 77 K or more[8], which would make them maintainable in interplanetary space using simple multi-layer insulation and highly reflective coatings. Assuming that this performance will someday be realizable in bulk cable, we can parameterize the problem of estimating potential magsail performance by assuming the availability of a high temperature superconducting cable with a critical current of 10^{10} Amps/m^2, i.e. equal to that of NbTi. Because the magnets are operating in an ambient environment below their critical temperature, no substrate material beyond that required for mechanical support is needed. Assuming a fixed magnet density of 5000 kg/m^3 (copper oxide), such a magnet would have a current to mass density (j/p_m) of $2.0x10^6$ Amp-m/kg.

By interacting with the Earth's magnetic poles, the magsail can generate sufficient force to allow it to drive both itself and a substantial payload up to escape velocity via a series of perigee kicks. Once escape has been reached, the magsail will find itself in interplanetary space where the solar wind is available to enable further propulsion. Such maneuvers are discussed in reference 13. In this report, however, we shall limit ourselves to discussing the operation of the magsail in a plasma wind. Such operations enable both maneuvering in heliocentric space and deceleration of ultra-high velocity interstellar spacecraft without the use of propellant. It also provides an option for lowering the orbit of a spacecraft by creating drag against a planetary ionosphere.

Magsail Theory

The Magsail Operating In A Plasma Wind

Two alternative methods have been used to analyze the performance of the magsail in a plasma wind. In the first, the particle method, the solar wind was viewed as an aggregation of particles each interacting individually with the vacuum magnetic field of the magsail. The magsail was first analyzed by Andrews and Zubrin in 1988 using this

model, and the results of that study are reported in reference 1. In the second model, the solar wind is viewed as a plasma fluid creating a supersonic shock as it impinges upon the magnetosphere of the magsail, much as occurs in the case of the interaction between the Earth's geomagnetic field and the solar wind. This second, plasma, model is probably a closer reflection of the actual behavior of the magsail. We will restrict ourselves to the plasma model in the presentation below. However because the ion cyclotron radius in the outer region of the magsail's magnetosphere (about 100 km) is comparable to the overall dimensions of that magnetosphere, the particle model has a certain amount of validity as well. The truth, no doubt, will be found somewhere between the two. Fortunately, the answers given by the two approaches are not at great variance.

Plasma Fluid Model

In the plasma fluid model, the magsail is approximated by a dipole field (or a collection of dipoles) compressed within a boundary created by a perfectly conducting plasma wind. Within the boundary, there is magnetic field but no significant plasma pressure; outside the boundary there is a plasma stream with significant dynamic pressure ($q = pV^2/2$) but no magnetic field. The boundary is taken to be the surface in space at which the magnetic pressure $B^2/2\mu = q\cos^2\varpi$, where ω is the angle between the free stream solar wind direction and the normal to the boundary surface[9]. This kind of interaction between the Earth's magnetosphere and the solar wind is depicted in Fig. 2.

The derivation and analysis of the fluid model was first presented in reference 2. It was found that, assuming a drag coefficient of unity for the area defined by the magsail's magnetospheric boundary, the drag exerted by the magsail, D, radius R_m, and current I is given by:

$$D = 1.175\pi(p\mu^{1/2}IR_m^2V^2)^{2/3} \qquad (1)$$

The mass of the magsail, M, with cross sectional area A and density p_m is

$$M = 2\pi R_m A\, p_m = 2\pi R_m I/(J/p_m) \qquad (2)$$

Taking the quotient of these two expressions, it was found that the self-acceleration of the magsail (without payload), D/M, is given by:

$$D/M = 0.59(\mu p^2V^4R_m/I)^{1/3}(J/p_m) \qquad (3)$$

Where J is the current density in the magsail wire and p_m is the density of material in the magsail

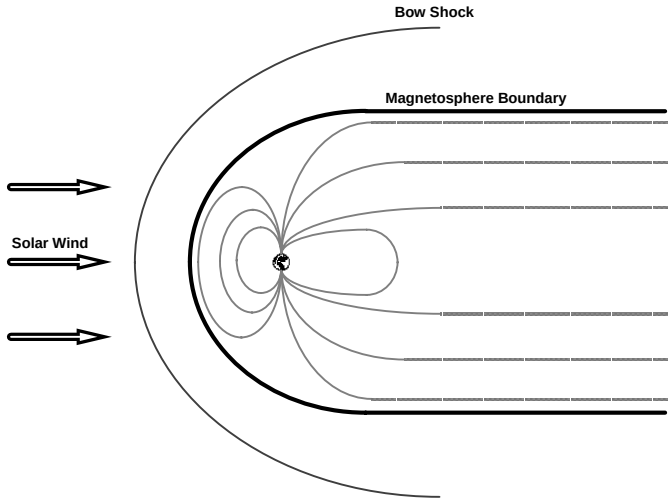

Figure 2. The Earth's Magnetosphere.

wire. If we substitute into this expression typical solar wind values of V = 5 x10^5m/s, p =(8.35 x 10^{-21}kg/m^3)/R_S^2, where R_S is the distance of the magsail from the sun in astronomical units, J/p_m = 2 x 10^6 amp-m/kg, and μ=4πx 10^{-7} N/amp^2, then the general equation (3) reduces for this particular case to:

$$D/M = 0.02(R_m/(IR_s^4))^{1/3}\ m/s^2 \qquad (4)$$

From expressions (3) or (4) it can clearly be seen that in the fluid model it is advantageous to construct the magsail with a small current (i.e. thin wire) but a large radius. Using equation (4) we find that for a sample magsail with B_m = 10^{-6} T, R_m = 31.6 km, I = 50 kA, wire diameter, d = 2.52 m, sailing at 1 AU has a mass of 5 metric tons and a self acceleration of 0.0172 m/s^2. This performance would be degraded on an actual spacecraft in proportion to the weight factor W, or the "weight ratio," which equals the mass of the magsail plus payload divided by the mass of the magsail. The total magnetic energy contained in this sail is about 80 MJ, and the hoop stress is 11,760 psi. Thus this magsail can be "inflated" (i.e. have its current built up) by a 10 kW_e solar panel power array in about 2.2 hours (although an intermediate step of charging a capacitor bank and then using it to rapidly bring the superconductor up to full current may be useful to allow for more rapid inflation[6]), and the magsail material can probably react the hoop stress without additional mechanical support. However, even if the ceramic superconductor had a tensile strength of zero, this hoop stress could be reacted by a reinforcement of high strength aluminum that would only add about 10% to the sail mass. Adopting this worst-case assumption, the reinforced magsail self-acceleration is found to be 0.015 m/s^2. A 10 kW_e (at 1 AU) power source can be built for a mass as low as 600 kg, and so could easily travel with the magsail, allowing the magsail to be recharged if for any reason it is shut off during the mission. For missions to the outer solar system a radioisotope thermoelectric generator, AMTEC, or dynamic isotope power system (DIPS) would be more appropriate.

In the plasma fluid model lift can also be generated if the dipole is situated with its axis at some orientation intermediate between the axial and normal configurations. Using a hypersonic aerodynamics code, reference 2 reported simple dipole configurations with L/D as high as 0.14. If compound magsails were adopted, consisting of two or more loops connected by a spar along their axes, more desirable magnetospheric boundaries could be obtained yielding a higher L/D.

Magsail Orbits in Heliocentric Space

Methods of analytically calculating magsail orbits in heliocentric space were first presented by R. Zubrin in reference 2. In heliocentric space the force generated by the magsail's interaction with the solar wind is much, much greater than that created by the interaction between the magsail and the Sun's magnetic field, and so it is the plasma wind results, previously presented, that are relevant here.

Magsail Orbits Without Lift

In order to calculate the orbit of a magsail spacecraft, we choose to parameterize the drag (thrust) generated by the magsail in the solar wind as a fraction of the sun's gravitational attraction on the spacecraft. The sun's gravitational acceleration $g_S = .006/R_S^2$, and the maximum magsail spacecraft acceleration $D/M = 0.015/(WR_S^{4/3})$, where W, the weight ratio equals the mass of the magsail plus payload divided by the mass of the magsail. The apparent fraction, α, of the sun's gravity operating on the spacecraft with its magsail operating at full current is then given by:

$$\alpha = (1 - D/(Mg_S)) = (1 - 2.5R_S^{2/3}/W) \qquad (5)$$

If $\alpha = 1$, the magsail is not operating. If α is between 1 and zero, the spacecraft acts as a body moving about a star whose mass is the fraction of the sun's mass represented by α. If $\alpha = 0$, the spacecraft feels no solar force and moves in a straight line; while if $\alpha < 0$, the spacecraft feels a net repulsion from the sun and moves away in a hyperbolic orbit.

Lets say our 5 ton magsail requires 1 ton of additional mass for shrouds, solar panels, avionics, etc., and we wish to use it to transfer a 41.5 ton payload (W=9.5) from Earth to Mars. Assume that the magsail is co-orbiting with the Earth but outside of its gravitational well. Using canonical units[13] such that $R_{Earth} = V_{Earth} = GM_{sun} = 1$, we can write:

$$E = V_{sc}^2/2 - \alpha/R = -\alpha/2a \qquad (6)$$

where E is the specific energy of the spacecraft, V_{SC} is its velocity about the sun in canonical units, R is its distance from the sun in AU, and a is the semi-major axis of its elliptical orbit. Since for a Hohmann transfer to Mars, 2a=2.52, we can solve equation (6)

for the required value of α (V_{SC} initially =1) to send the spacecraft onto such an orbit. The result is $\alpha = 0.8289$. Checking equation (5) we find our spacecraft with W=9.5 is can attain an α at 1 AU as low as 0.7368, so it is capable of doing this maneuver. Since in this zero-lift trajectory angular momentum about the sun is conserved, upon reaching Mars orbit, the ship will be moving with a velocity of V_{SC}(Mars arrival) = 1/1.52 = 0.6579. If we now wish to circularize the orbit, we use this value of V_{SC} together with 2a=3.04 in equation (6) and find that the required value of α to circularize at Mars is 0.6579. Checking equation (5), we see that our spacecraft at 1.52 AU is capable of generating α as low as 0.652, and so it can circularize at Mars.

Our spacecraft is now moving in Mars' orbital track about the sun, but *at a different speed than Mars*. Mars is overtaking the spacecraft with a relative velocity of 4.564 km/s. This odd situation gives the magsail craft a very interesting capability. What it means is that the spacecraft can leave Earth for a Hohmann transfer to Mars' orbit, circularize, and then loiter at will in Mars' orbit until the Red Planet catches up to it. Thus a magsail interplanetary transfer can be done *at any time*, unlike ballistic interplanetary transfer orbits, there are no limited launch windows.

When Mars approaches, the magsail can release its payload, consisting of cargo plus an aerobrake, allowing the payload to aerobrake into Mars orbit or land. Simultaneously, the magsail reduces its current partially so as to increase α back to 0.8289, sending it on a Hohmann transfer orbit back to Earth. Upon reaching Earth orbit, the magsail is turned off, and the spacecraft will circularize at 1 AU. If the timing of this maneuver is incorrect for Earth rendezvous, all the magsail has to do is make its initial return Hohmann transfer to a circular orbit intermediate between Earth and Mars. The magsail can then waste as much time as required in that orbit to allow the Earth to attain the correct position for the final Hohmann transfer home. Since the intermediate orbit can be chosen at will, such return flights can be scheduled with great flexibility.

The time of flight of such magsail Hohmann transfers is given by:

$$t = \pi(a^3/\alpha)^{1/2} \qquad (7)$$

For our Earth-Mars Hohmann transfer, a=1.26, α=0.8289, and thus t=4.88 canonical units=283 days, a time slightly longer than the usual Hohmann transfer ballistic flight time.

Magsail requirements and capabilities are shown in Table 1 for moving payloads to different planetary destinations in the outer solar system, assuming no magsail lift. In Table 1., α_{trans} is the value of α required to initiate the transfer ellipse to the given destination, α_{circ} is the value of α required at that destination to circularize the orbit, α_{circ0} is the value that α would have to have been at 1 AU to allow the spacecraft to attain α_{circ} at the destination, W_{trans} is the weight ratio (the mass of the magsail plus payload divided by the mass of the magsail) allowable to permit the attainment of α_{trans}, and W_{circ} is the weight ratio allowable to permit the attainment of α_{circ0}. The weight

ratio actually attainable for any given destination is simply the lesser of W_{trans} and W_{circ}. We can see that a magsail without lift can move a payload amounting to 4 times the sail weight to any destination in the outer solar system.

Finally, if we do not desire to go anywhere in particular, but only wish to rapidly accelerate out of the solar system (as is required for the proposed Thousand Astronomical Unit[11] probe, for example) we can set W=1.25, and thus α=-1 at 1 AU, becoming more negative as we move out. Integrating the equations of motion, we find that the probe will be hurled out of the solar system with a terminal velocity of 95 km/s, reaching 1000 AU in about 50 years.

Table 1. .Zero Lift Magsail Payload Capability

Destination	α_{trans}	α_{circ}	α_{circ0}	W_{trans}	W_{circ}
Mars	0.8289	0.657	0.741	14.60	9.66
Jupiter	0.5906	0.192	0.711	6.11	8.64
Saturn	0.5525	0.105	0.801	5.58	12.55
Uranus	0.5259	0.052	0.868	5.27	18.96
Neptune	0.5165	0.033	0.900	5.17	25.06
Pluto	0.5125	0.025	0.916	5.12	29.87
Escape	0.5000	0.000	1.000	5.00	infinite

Magsail Orbits Utilizing Lift

If lift can be generated, the magsail becomes capable of changing its angular momentum about the sun, giving it both greater maneuverability and payload hauling capability. The mathematics of the orbit transfer becomes more complex. Methods of calculating such orbits were derived by R. Zubrin in 1989 and are given in reference 2.

The use of lift allows for the magsail to adopt much more flexible flight plans between planets. For example, let us say we send the spacecraft on a zero-lift trajectory towards Mars. We arrive in Mars orbit, and dally until Mars shows up, at which point we release the payload and set forth on a transfer orbit towards Earth, all as described in the discussion of zero-lift maneuvers. Now, however, we apply negative lift to decrease the spacecraft's angular momentum about the sun. In this case, when we arrive at Earth orbit, we need a value of $\alpha < 1$ to circularize, which means that we can now circularize in *Earth* orbit with a different orbital velocity than the Earth, and loiter until the Earth catches up to us. We thus have the ability to move large payloads back and forth between the Earth and Mars with the knowledge that rendezvous can be achieved at each end of the orbit without regard to when the spacecraft sets forth. This solves the problem that derailed the concept of cycling interplanetary "castles" i.e. the inability of these large manned habitats following ballistic interplanetary orbits to obtain a useful number of planetary encounters in their lifetime[12]. In effect the magsail allows the castles to "cheat" against the laws of orbital mechanics by giving it the ability to adjust the effective mass of the sun to that required to assure orbital rendezvous with the target planet at each end of the castle's commute. In addition, the use of negative lift allows the magsail to drop below Earth orbit to visit Mercury and Venus.

If lift is to be utilized, it becomes necessary to be able to control the orientation of the magsail. One way to accomplish this would be to connect the payload to the magsail loop with a set of tethers that can be either reeled in or out on a windlass. This would allow the magsail to shift its center of mass in either of the two dimensions within the plane of the loop. By moving the center of mass relative to the sail's center of pressure a torque can be induced, allowing the magsail to be swung into the desired attitude.

Above and beyond its propulsive capability, the magsail has an additional advantage as a system for manned interplanetary spacecraft, in that it shields the crew from a large portion of the radiation dose they would otherwise receive from the solar wind and solar flares. Without such shielding, these hazards may well place a constraint on long distance manned spaceflight.

Magsails can also be used to generate thrust within a planetary magnetosphere by pumping against a planet's magnetic poles. Such use is discussed by Zubrin in reference 13.

The Magsail as an Interstellar Brake

In addition to its role as an interplanetary propulsion system, the magsail also offers great potential as the braking device[1] for an interstellar spacecraft that has been previously accelerated to very high velocities by some other means, for example by a fusion rocket or a laser pushed lightsail. In this case, the plasma wind is the apparent wind created by the relative velocity between the spacecraft and the interstellar medium. In reference 1, the particle model was used to show that a relativistic magsail could brake itself with an e-folding velocity decay time of 36 years, if $J/p_m = 2.0 \times 10^6$ amp-m/kg. A more accurate and a more favorable result can be derived utilizing the plasma fluid model. Using equation (3) with $V=V_{SC}$, $p=1.67 \times 10^{-22}$ kg/m^3, R_m = 100 km, I = 159 kA, and W =2 (a 50 ton magsail with a 50 ton payload), we obtain:

$$dV/dt = -1.66 \times 10^{-11} V^{4/3} \qquad (8)$$

The solution of this equation is:

$$V = V_0/(1 + 3.68 \times 10^{-12} V_0^{1/3} t)^3 \qquad (9)$$

where V_0 is the velocity of the spacecraft at the beginning of the braking maneuver. If V_0 is 3×10^7 m/s (one tenth the speed of light) and t is given in years, (9) becomes:

$$V = (3 \times 10^7 \text{ m/s})/(1 + 0.054t)^3 \qquad (10)$$

which will reduce V by a factor of 8 in 18.5 years. In 55.5 years V will be reduced by a factor of 64 to 468 km/s, a velocity suitable for magsail or fusion rocket braking within the destination solar system itself. For all intents and purposes, the magnetic sail has

eliminated the propellant required for terminal deceleration, with the result being an enormous reduction in mission mass ratio.

The above calculation (as well as the calculations in reference 1) are based on an assumed interstellar hydrogen number density of $10^5/m^3$. This is quite conservative. Some astronomers put the estimate ten times higher, which would shorten the time scales given above by a factor of 4.64.

The Phase I Study

As can be seen from the above, the mathematics for calculating potential magsail performance has been worked in considerable detail. These theoretical results clearly show that the magsail has enormous potential to revolutionize humanity's spaceflight capabilities; allowing propellant-free transfer of large payloads throughout the solar system and potentially enabling interstellar flight.

In order to more adequately explore the technology, design and operability issues that will determine if this very promising technique for space propulsion is feasible, Pioneer Astronautics proposed a Phase I investigation. This study, which was approved by the NASA Institute of Advanced Concepts (NIAC) took an in-depth look at magsail technology, design, and operations, and also defined a Phase II experimental program to move magsails from their current concept stage to flight demonstration. Some of the most important results of that study are presented below.

Perhaps more than any other driver, it is absolutely essential to utilize a superconductor with a sufficiently high current density to mass ratio and high operating temperature in order to minimize magsail mass. (Zubrin, Andrews) [1-3] Therefore, in the first phase of this project, research was conducted to determine the ability of present and probable future superconductor technology to meet these requirements. Design and performance issues are then discussed, including operation in near-solar, interplanetary, and interstellar space. A description of a magsail development program rounds out this report, with simulations and experiments designed to further magsail technology.

Superconductor Trade Study:

To obtain the lowest total superconducting coil mass, and thus the highest MagSail acceleration/highest payload capacity, it is desirable to have:

1) The **lowest cable density** possible, to cut down on cable mass.

2) The **highest critical temperature** possible, to allow passive rather than active cooling, if possible, and minimize thermal control systems mass.

3) The **highest current density** possible (and ultimately the highest engineering critical current density possible) to maximize cable thrust.

Terms:

H_{c2} - Upper critical field: maximum magnetic field a superconducting material can withstand before entirely losing its superconductivity.

I_c - Critical current: maximum current a superconducting material can carry before losing its superconductivity. Can be measured according to different criteria, the commonly used resistive method measures voltage difference of 1μV/cm.

J_c - Critical current density: critical current divided by cross-sectional area of current carrying superconducting material, often a filament imbedded in a larger non-superconducting matrix, a thin-film on top of a thick non-superconducting substrate or a fraction thereof. Method by which J_c is measured is not always uniform between labs. The critical current density decreases very rapidly with increasing temperatures and magnetic fields.

J_e - Engineering critical current density: critical current divided by the total cross-sectional area of wire, tape, or structure of interest, including non-superconducting substrates.

T_c - Critical temperature, the highest temperature at which a superconductor can function without losing it superconductivity.

BSCCO - Barium Strontium Copper Calcium Oxide
HBCCO- Mercury Barium Copper Calcium Oxide
TBCCO- Thallium Barium Copper Calcium Oxide
YBCO - Yttrium Barium Copper Oxide

Superconducting Wire Density:

Because presently available long-length wires are mostly metal, their mass densities are roughly similar, $9.2x10^3$ kg/m^3 for high temperature silver BSCCO Bi-2212 wires, which can operate above 90 K (Motowidlo, IGC)[16] to ~$6.5x10^3$ kg/m^3 for low temperature wires, operating below 20 K, with densities assumed to be halfway between that of Nb and Ti [17] (CRC) .)

Research is being done to produce high-temperature tapes based on a Ni-alloy substrate, which would be expected to be under $8.90x10^3$ kg/m^3, the density of pure Ni.[17]

In the future, as high temperature superconductor wires are improved, it is assumed their metal content will decrease, with mass density falling from $9.2x10^3$ kg/m^3 (BSCCO Bi-2212) towards $5x10^3$ kg/m^3 (pure copper-oxide).[1]

Therefore, *critical temperature and critical current density become design drivers over mass density for presently available materials.* In the present, low temperature materials may be somewhat lighter, in the longer term high temperature superconductor mass densities should be about the same or a little less.

Superconducting Critical Temperature and Current Densities:

Low Temperature Superconductors:

The best Low Temperature Superconductors have good current densities, 10^{10} to ~10^{11} A/m^2 at 2.7 K [1], with J_c's 3-5 times lower for conductors at 4 K.[18] However low temperature superconductors can't operate above 18.1 K. Niobium-Titanium and Niobium-Tin are commonly used in wires and high strength magnets in specialty applications such as MRI's and particle accelerators.

Niobium Titanium:

NbTi has a J_c of 3×10^9 A/m^2 (at 5 T, 4.2 K)[18], which increases to 4.25×10^9 A/m^2 for specially processed artificial pinning center wire (at 5 T, 4.2 K).[19] It has a T_c of 9.2 K and a H_{c2} of 11 T. [20,21]

Niobium Tin:

Nb_3Sn has a J_c of $1\text{-}2 \times 10^9$ A/m^2 (at 10 T, 4.2 K).[18] It has a T_c of 18.05 K [22] and a H_{c2} of 24 T. [21]

High Temperature Superconductors:

High Temperature Superconductors were first discovered in 1986, with La compounds operating at 35 K.[23] The best HTS materials can now operate much higher, up to 135 K (164 K under high-pressure [24]) and small samples can exceed critical current densities of 10^{10} A/m^2, with performance typically a magnitude better at lower temperatures. The biggest problem is growing and precisely aligning the crystals of HTS materials in large scale manufacturing processes so that the same performance found in small thin-film crystals can be approached. These HTS materials are anisotrophic in response to magnetic fields with degraded performance as fields increases. Present BSCCO superconductors experience significant "flux creep", or movement of magnetic flux lines. Flux creep absorbs energy and can cause the persistent current in a superconductor to decay 30-40% in 2-4 hours, even with no applied external magnetic fields.[25] This may necessitate a quick charge rate for the demonstration sail, continuous trickle charging, and increased heat dissipation. These modifications are assumed to be small and have not been analyzed further. YBCO and future BSCCO may have a higher resistance to flux creep, and may be amenable to longer charge times with less topping off of current.

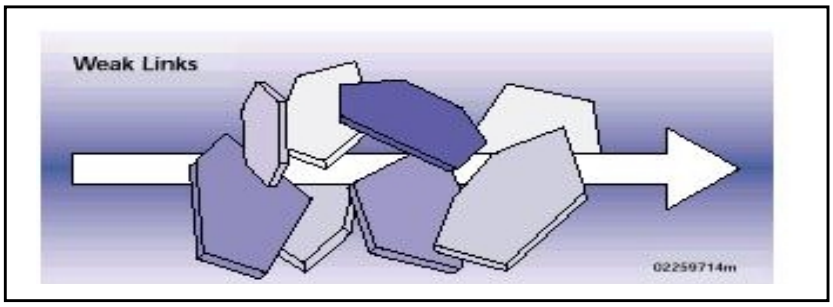

Fig 3. Weak Links, poorly aligned crystals (DOE)[23]

The most popular HTS compounds are BSCCO and YBCO.

Critical current densities are commonly reported at 77 K and zero applied magnetic field, which is used in this report unless otherwise stated.

Barium Strontium Calcium Copper Oxide:

Barium Strontium Calcium Copper Oxide, BSCCO, is currently the only HTS compound made into long wires but its ultimate (single-crystal) J_c (at 0T, 77 K) is a magnitude less than that of YBCO. It has a T_c of up to 110 K and a H_{c2} (at 77 K) of 3.5 /35 T (**(||,** ⊥ to the crystallographic axis, c). At 4.2 K, the H_{c2} is 29/400 T (**||,** ⊥ to the c-axis).[21]

The Bi-2122, phase of BSCCO has a J_c of ~7 x 10 ^{9} A/m^2 for a single-crystalline thin film (at 0T, 60 K)[26] with its highest T_c at 95 K. [21]

The Bi-2223, phase of BSCCO, has a J_c of ~ 10^{10} A/m^2 for a single-crystalline thin film (at 0T, 77 K).[27] Its highest T_c is ~ 107 K. [18]

BSCCO wire is made commercially by the powder-in-tube (OPIT) process by American Superconductors, Intermagnetics General Corporation, and others. The OPIT process is used in order to self-align the BSCCO crystals and add oxygen, but this requires an expensive and massive matrix of Ag, which limits its potential engineering critical current density. Presently, the highest engineering critical current density is for BSCCO Bi-2223 OPIT wires from American Superconductor. They have reached a record J_e of 1.12x10^8 A/m^2 for wires over 200 meters long , averaged over 100 samples, and a maximum J_e of 2.3 x10^8 A/m^2 for shorter 10 cm long wires.[24]

As BSCCO wires improve, they will become more useful, but they still fall short of the performance that YBCO could deliver.

Yttrium Barium Copper Oxide:

YBCO, has reached a peak J_c of 10^{11} A/m^2 for a thin-film deposited on Strontium Titanate single crystals [28]. YBCO has a T_c of up to 92 K and a H_{c2} (at 77 K) of 9/56 T (**||,** ⊥ to the crystallographic axis, c) At 4.2 K, the H_{c2} is 55/290 T (**|| ,**⊥ to the c axis).[21]

Thin films have also been deposited on a Nickel substrate with a J_c of 3x10^{10} A/m^2 at the Oak Ridge National Laboratory, using a patented Rolling-Assisted Biaxially Textured Substrate, (RABiTS) process [29] The RABiTS process is exciting because it is the kind of process that could be scaled up to make industrial quantities of thin-film based wires from YBCO or other HTS materials, such as TBCCO. (Whereas the OPIT process only works for BSCCO.)

Other processes could also be used such as Ion-beam deposition (IBAD) and Combustion Chemical Vapor deposition. IBAD can grow thin-films, but requires the alignment of a template layer, which is a very slow process <0.1 nm/sec. [18] Combustion Chemical Vapor deposition, researched by MicroCoating Technologies and Oak Ridge National Lab, could also grow thin-films on Ni wires but has yet to match the performance of RABiTS.[30]

Mercury Barium Calcium Copper Oxide

Mercury Barium Calcium Copper Oxide, HBCCO, is toxic and doesn't have a J_c as good as YBCO, but it has the highest critical temperature, 135 K (164 K under high-pressure). New formulations and processes could make HBCCO or HBCCO related compounds more useful. [31]

Thallium Barium Calcium Copper Oxide

Thallium Barium Calcium Copper Oxide is also toxic and its J_c is about $3x10^{11}$ A/m^2, [31] with itsTl-2223 phase at a J_c of $3.25x10^{11}$ A/m^2 (spray pyrolyzed on ceramic).[32] TBCO's critical temperature is 110-128 K. [31] New formulations and processes could make also TBCCO or TBCCO related compounds more useful.

Superconducting Technology: What Can We Expect ?:

It is not currently possible to know if a wire with $J_e = 1.0 \times 10^{10}$ A/m^2 will ever become available in long lengths, but we have reasons to be optimistic.

The highest engineering critical current density yet reported for a commercial superconducting wire is for BSCCO-2223 OPIT wire from American Superconductor, with a J_e of $1.12x10^8$ A/m^2 for wires over 200 meters long (averaged over 100 samples) and a maximum J_e of 2.3×10^8 A/m^2 for shorter wires, 10 cm long.[24]

John Cerulli, Applications Engineer of American Superconductor, Westbourough, MA predicts progress in commercial BSCCO wire to follow a linear trend, Malozemoff's law. (See Fig 4) [34] If this trend continues, one can extrapolate a J_e of $1.76x10^8$ A/m^2 in 2005, a J_e of $2.1x10^8$ A/m^2 in 2010, and a J_e of $2.4x10^8$ A/m^2 around 2015 for BSCCO wires over 100 meters long. However, as previously mentioned, other HTS materials are being explored as thin films, and could lead to greater performance.

Dean Peterson, Leader of the Superconducting Technology Center at the Los Alamos National Laboratory has speculated that given adequate funding and continued progress, "..it would not be unreasonable.." to reach a J_e of 10^9 A/m^2 in 5 years, a J_e of 10^{10} A/m^2 in 10 years, and a J_e of 10^{11} A/m^2 in 15-20 years in tapes or wires made from thin films. In fact, Los Alamos has already made a one meter long thick-film tape of YBCO on a Nickel alloy substrate with a J_c of 1.2×10^{10} A/m^2 (at 77K) and plans to lengthen it to 10 meters with the help of industry.[28] The prediction of a J_e of 10^{11} A/m^2 in 20 years, (LANL), is compared, in Fig 5, to American Superconductor's linear trend for BSCCO wires, (ASC).

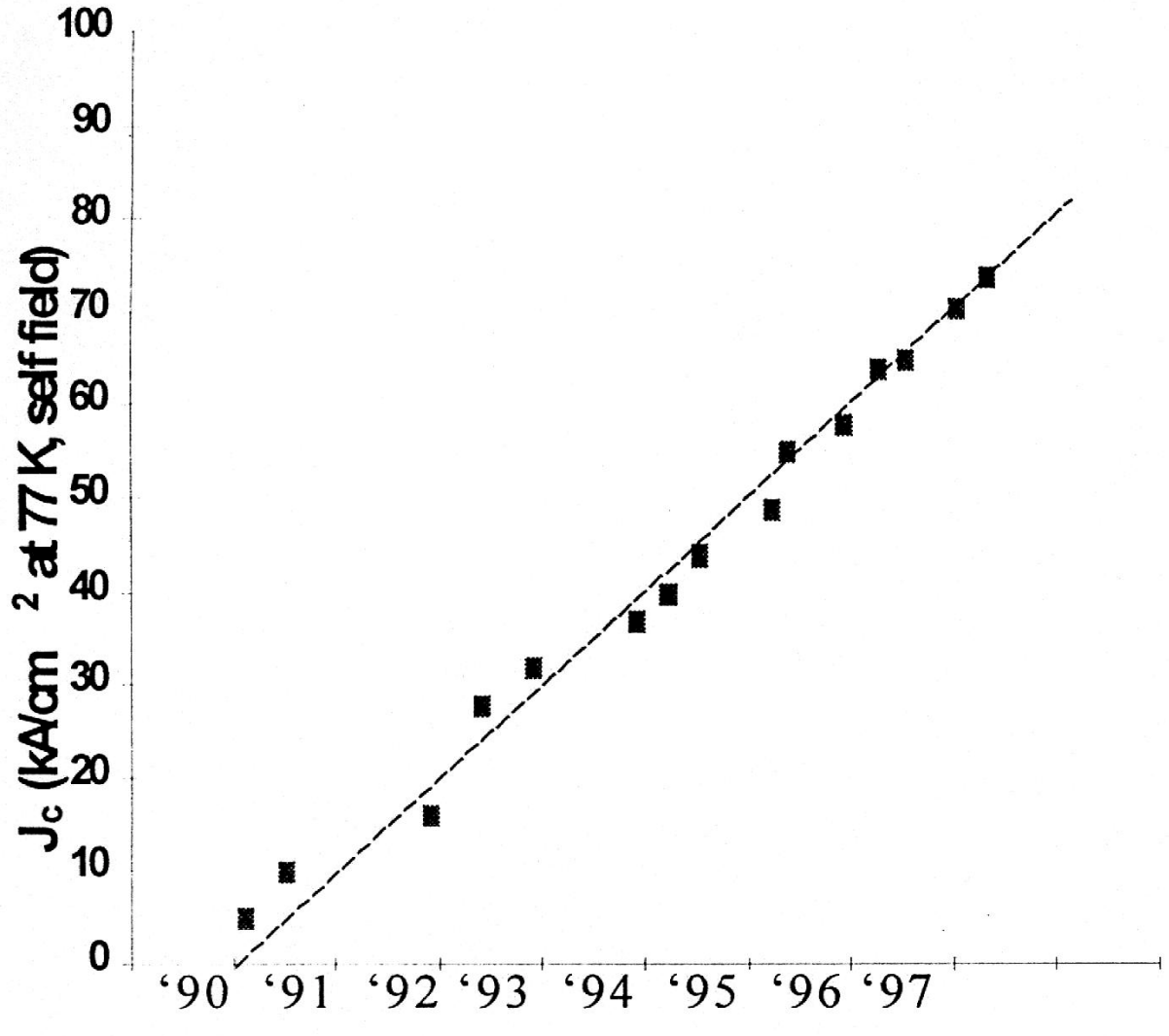

Fig 4: Malozemoff's Law for BSCCO Bi-2223 (Cerulli)[34]

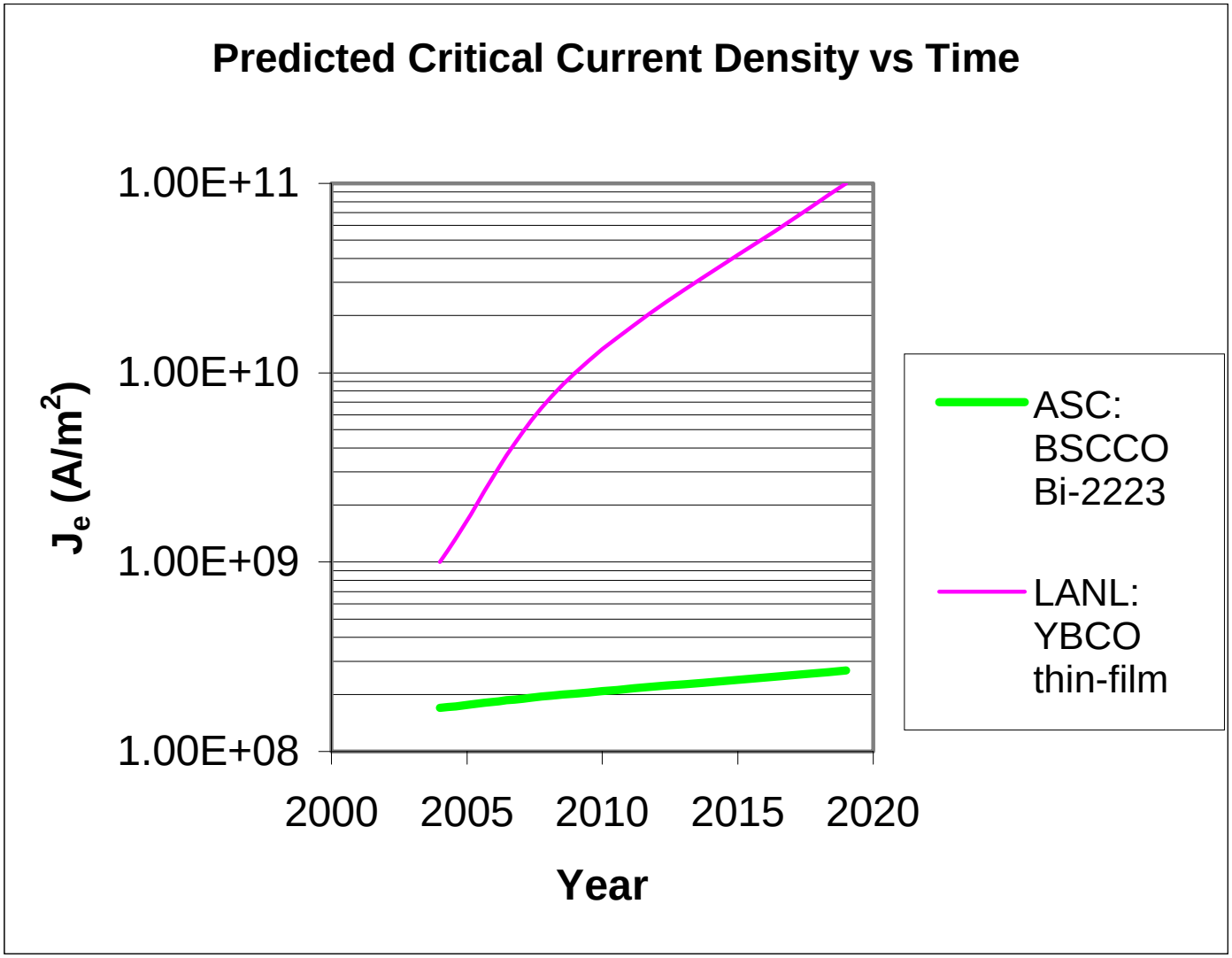

Fig 5: Critical Current Density Predictions (77K, 0 T) for commercial long length wires, L > 100 m.

Robert Hawsey, Director of Superconductivity Technology at the Oak Ridge National Laboratory, also agrees that a J_e of 10^9 A/m^2 would be a good five year goal, but was unable to speculate further.[35]

Dr. Hawsey stated that in order to reach a J_e of 10^{10} A/m^2 it would be necessary to increase amount of HTS material in tape dramatically from current value of 2% and develop industrial processes to make long lengths of tape (on a continuous basis). [35] Paul Berdahl, thin film researcher at Lawrence Berkley Laboratory, believes that, "a 10^{10} A/m^2 (J_e) film wire is allowed by knowledge..", though technical problems exist in superconductor material deposition, manufacture of the substrate.[36]

Some processes, such as IBAD and RABiTS, seem to be headed in this direction, but, considering the difficulty of aligning HTS grains (within 10 degrees) it will take significant work and time and funding to continue progress. Not everyone has an equally optimistic short-term projection. Dick Blaugher of the National Renewable Energy Laboratory, thinks Los Alamos is unlikely to have long wire with a J_e of 10^9 A/m^2 in five years [37], but like many other researchers, did not wish speculate farther into the future.

Table 2. Peak Critical Current Densities Summarized (in A/m^2)

	J_c at 77 K	**J_e* at 77 K**	**Predicted J_e in 10 years at 77 K**
BSCCO	7×10^9	1.4×10^8	2×10^8
YBCO	10^{11}	2×10^9	10^{10}
HBCCO	$<10^{11}$	$< 2 \times 10^9$	----------
TBCCO	3×10^{11}	6×10^9	----------

*Assumed to equal $J_c/50$, ie. 98% substrate

Conclusions of Superconductor Trade Study:

The performance, current-density to mass-density ratio, of the best available superconducting wire, American Superconductor's BSCCO Bi-21223-OPIT wire, is two orders of magnitude below the value assumed for practical applications by Zubrin and Andrews. It is however sufficient for a proof-of-concept demonstration. As shown by Zubrin and Andrews in earlier studies, a magsail's acceleration can be treated as effectively reducing the solar gravity to fraction of its original value, α, resulting in an orbit with a new semi-major axis and apoapse. The acceleration without payload, self-acceleration, is calculated using equation 1, and , α is calculated from the canonical orbit equation $-\alpha/2a=V^2/2-\alpha/R$ (where R=V=1 for Earth, and a= semi-major axis in au). A current state-of-the-art MagSail with no payload could obtain an, α of 0.9698 and an aphelion of 1.064 AU. Near term advances in YBCO thin-film wires should allow an aphelion greater than 1.067 AU. Even without other performance boosting techniques, described later in this report, such advances should be more than adequate for a demonstration flight to a Near-Earth Object.

In five years, wire current density could be within a magnitude of Zubrin and Andrews' baseline value. With a small reduction in mass density from current values, such a wire would allow a MagSail, without payload or support structure, to compete with solar sails. The acceleration would rise to 8.85×10^{-4} m/s^2 and the aphelion would increase to 1.42 AU , nearly to Mars!

The ultimate performance of a MagSail, based on YBCO thin-film, could exceed the base-lined J_e (10^{10} A/m^2) by an order of magnitude for interplanetary travel and perform two orders of magnitude better at the low temperatures of interstellar space.

Table 3 compares magsail present and predicted performance as a function of current density.

Equation 1:[2]

Self-acceleration (acceleration of cable without payload) = D/M

$$\mathbf{D/M = 0.59\ (\mu\rho^2 V^4 R_m/I)^{1/3}(J/\rho_m)}$$

Where:

$\mu = 4\ \Pi \times 10^{-7}\ N/A^2$ (Vacuum permittivity constant)
$\rho = 8.35 \times 10^{-21}\ kg/m^3$ (Solar wind density)
$V = 5 \times 10^5\ m/s$ (Solar Wind speed)
R_m in km (MagSail loop radius)
$I = 5 \times 10^4$ Amps (MagSail loop current)
ρ_m= in Kg/m^3 (Magsail coil density)

TABLE 3: Magsail Missions

Magsail Radius	Current Density	Wire Density	Self-Accel.	α	Semi-major axis	Aphelion	Comments:
(m)	(A/m^2)	(Kg/m^3)	(m/s^2)		(au)	(au)	
3.16E+04	**2.30E+08**	**9.00E+03**	**0.000181**	**0.9698**	**1.0321**	**1.0642**	**Best Available BSCCO**
3.16E+04	**2.40E+08**	**9.00E+03**	**0.000189**	**0.9685**	**1.0336**	**1.0672**	**Near-Term YBCO Tape [a]**
3.16E+04	**1.00E+09**	**8.00E+03**	**0.000885**	**0.8524**	**1.2094**	**1.4187**	**5 year YBCO Prediction [b]**
3.16E+04	**1.00E+11**	**5.00E+03**	**0.141666**	**-22.6110**	**∞**	**∞**	**YBCO Ultimate (present thin-film max) [b]**
1.28E+04	*2.00E+10*	*1.00E+04*	*0.022489*	*-2.7482*	**∞**	**∞**	*Lunar (multiple coils)*
3.16E+04	*1.00E+10*	*5.00E+03*	*0.017849*	*-1.9748*	**∞**	**∞**	*Planetary*
1.00E+05	*1.00E+10*	*5.00E+03*	*0.003996*	*0.3340*	**∞**	**∞**	*Interstellar*
1.00E+05	*1.00E+11*	*5.00E+03*	*0.039960*	*-5.6601*	**∞**	**∞**	*Interstellar Adv.*

[a] Assumes a $J_e = .02$ of J_c, roughly proportional to present HTS/substrate ratio.
[b] Assumes a drop in wire density.

α = 1 – (Self-Acceleration/Solar Gravitational Acceleration of $6 \times 10^{-3}\ m/s^2$)

Magsail Systems Design

Baseline Magsail Designs

For purposes of engineering analysis, two baseline magsails were proposed as part of the present study. The first, the Demonstrator, is a 200 m radius, 90 kg unit utilizing state of the art BSCCO wire capable of moving a 10 kg payload from 1 AU to 1.027 AU. This has limited practical value but would effectively demonstrate magsail technology. The Operational magsail is a 20 km radius, 10.8 tonne spacecraft employing relatively near-term YBCO technology capable of moving a 11 tonne payload from 1 AU to Mars in a direct flight. Such a spacecraft obviously would have great utility. The requirements of these two spacecraft designs were assessed in the engineering studies below.

Coil Geometry Trade Study:

Introduction:

Because current density increases as temperature decreases, it is essential to keep the coil temperature as low as possible to attain the maximum current density. It is also necessary to use lightweight material to minimize total magsail system mass and maximize performance.

.

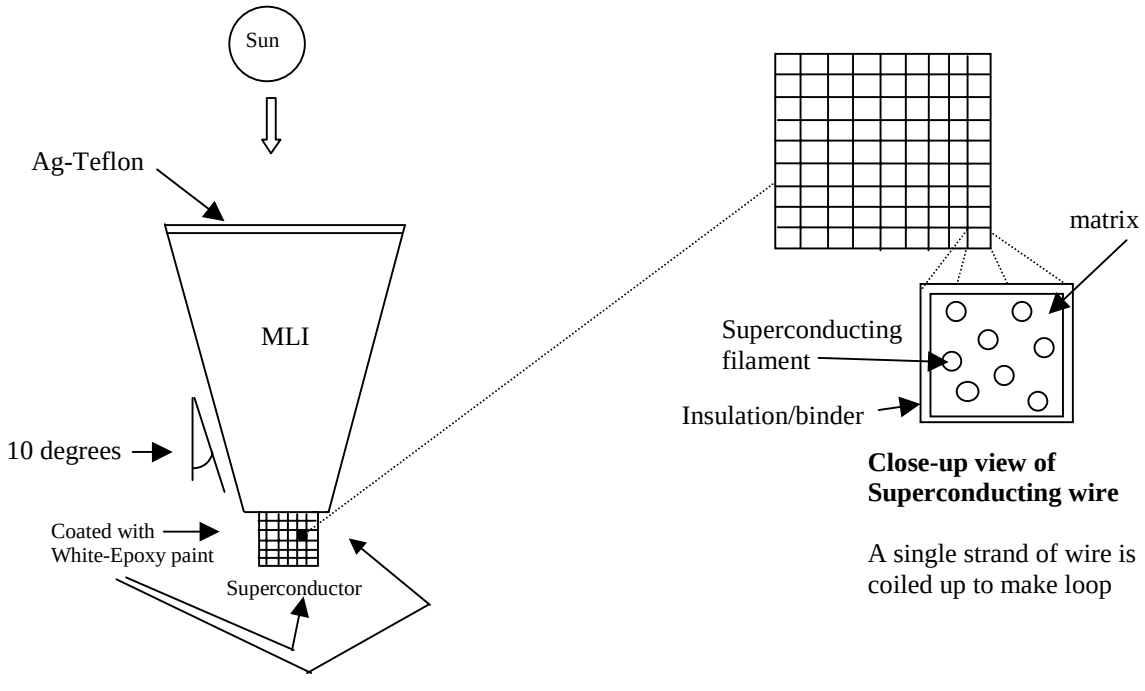

Fig 6: Cable Geometry

The main coil consists of a loop of superconducting wire, covered with Multi-layer insulation (MLI) with a wedge-shaped cross-section The layers of MLI widen closer to the top, to act as a sunshade. The top layer of MLI is coated Silvered-Teflon (Ag-Tef.). The bottom layer of MLI and the exposed surfaces of the wire are coated with white epoxy paint to increase the thermal energy radiated into space and minimize temperature.

These materials were chosen to allow the wire to cool to the lowest possible temperature, using current lightweight materials. Due to the geometry of the MLI, the cable will have a pointing margin of ± 10 degrees. (See Fig 6)

Results:

A wire with a square cross-section wire was chosen for ease of manufacture and compact size. Maximum temperatures were determined from the Thermal Transport Equations **(see next page).**

The temperature of the Ag-Teflon coated upper surface was approximated as 305.8 K, hot enough to radiate all solar energy absorbed by the aged Ag-Teflon. This maximum was used as the starting temperature for the top of the first MLI layer.

Before the Ag-Teflon surface ages (9 months to 4 years), its temperature will be colder than 305.8 K. Its (fresh) solar absorptivity of 0.08 will asymptotically increase to 0.241, the value used in calculations. [38]

MLI performance was modeled as several 1 mm thin layers. In each layer, temperatures were estimated by setting the energy conducted through the layer per m^2, $(k \Delta T)/\Delta X$, equal to the energy radiated away by the bottom of the layer per m^2, $\varepsilon \sigma_{Bc} A_{sf} T^4_{\text{MLI bot}}$. The calculations used the Fick's Law approximation to radiative transfer (Lockheed Correlation) which has been shown to accurately model radiative transfer in MLI coverings in many past aerospace industry studies.

Each layer has a shape factor, $A_{sf, to}$ account for heat loss through the sides. The shape factor is equal to the area of the sides and bottom of the MLI layer divided by the area of the top of the MLI layer. Both the area intersected by the wire and MLI (with the emissivity of the white epoxy) and the area of the MLI sides (with the emissivity of Aluminum) was used to calculate the temperature of the bottom of the lowest MLI layer and the temperature of the wire. The wire was assumed to be in thermal equilibrium with the lower side of the bottom layer of MLI and with its white epoxy coating (see Fig. 7: Calculating MLI Areas and Table 4: Thermal Transport Equations on next page)

Fig 7: Calculating MLI Areas:

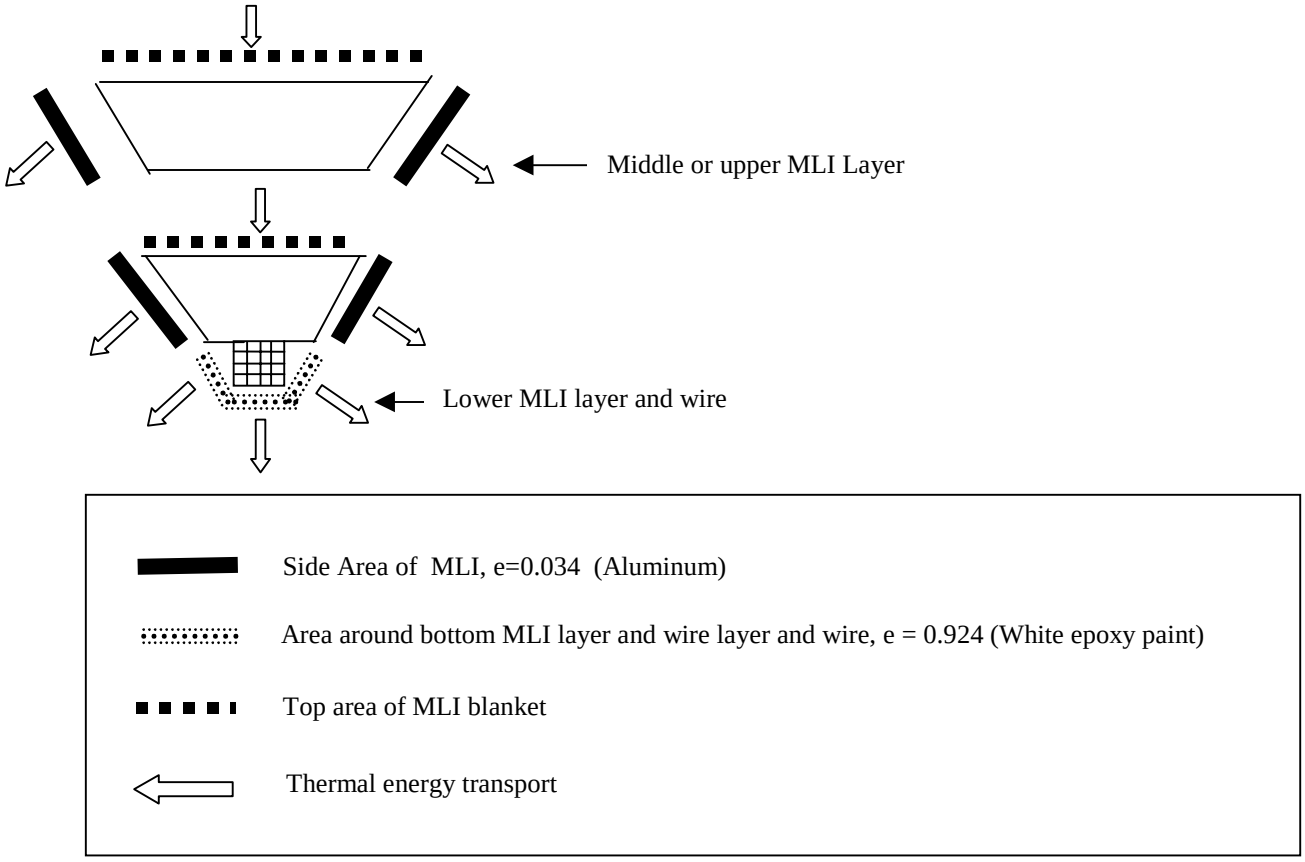

Table 4: Thermal Transport Equations[38]

α = solar absorptivity
(EOL- End of life value used for Ag-Teflon, 0.241 instead of .08
A_{sf} = area shape factor = area of top MLI layer/ effective radiating area of bottom layer, including side losses.
ε = emissivity *($\varepsilon_{AL} = 0.034$, $\varepsilon_{White\ Epoxy} = 0.924$, $\varepsilon_{Ag\text{-}Teflon} = 0.66$)*
k = Thermal conductivity of MLI =6.3 x 10^{-5} w/m K
SC = Solar constant = 1358 W/m^2 at 1 AU
σ_{Bc} = Stephan-Boltzman Constant = 5.67 x 10^{-8} w/m^2K^4
Q_1= Energy from Sun absorbed by Ag-Teflon per m^2 (Top MLI surface)
Q_2= Energy emitted by Ag-Teflon per m^2 (Top MLI surface)
$T_{1\ max}$ = Maximum temperature of Ag-Teflon
$T_{MLI\ Top}$= Temperature of the top of a layer of MLI
$T_{MLI\ bot}$= Temperature of the bottom of a layer of MLI
ΔX = thickness of MLI layer

$Q_1 = A_1\ \alpha_1\ SC$
$Q_2 = A_2\ \varepsilon_1\ \sigma_{Bc}\ T_1^4$
$T_{1\ max} = [\ \alpha_1\ SC/\varepsilon_1\ \sigma_{Bc}\ T_1^4\ ]$
$T_{MLI\ bot} = T_{MLI\ Top} + (\ \Delta X\ \varepsilon_{AL}\ \sigma_{Bc}\ A_{sf}/k)\ T_{MLI\ Top}$ -- for middle MLI Layer
$T_{MLI\ bot} = T_{MLI\ Top} + (\ \Delta X\ \sigma_{Bc}\ (\varepsilon_{AL}\ A_{sf\ MLI\ side} + \varepsilon_{Epoxy}\ A_{sf\ lower\ MLI\ surface\ and\ exposed\ Wire})/k)\ T_{MLI\ Top}$ -- for bottom MLI Layer

Thermal Analysis Results:

The calculated temperature (Fig 8) of the magsail wire decreases as MLI thickness increases, with the most pronounced drop occurring in the first few layers. As the wire temperature drops, current carrying ability increases. At approximately 18 layers, the performance gain from thicker MLI, and colder superconducting wire levels off due to mass increase. (Assuming a linear relationship in J_e vs. T similar to BSCCO, described later.)

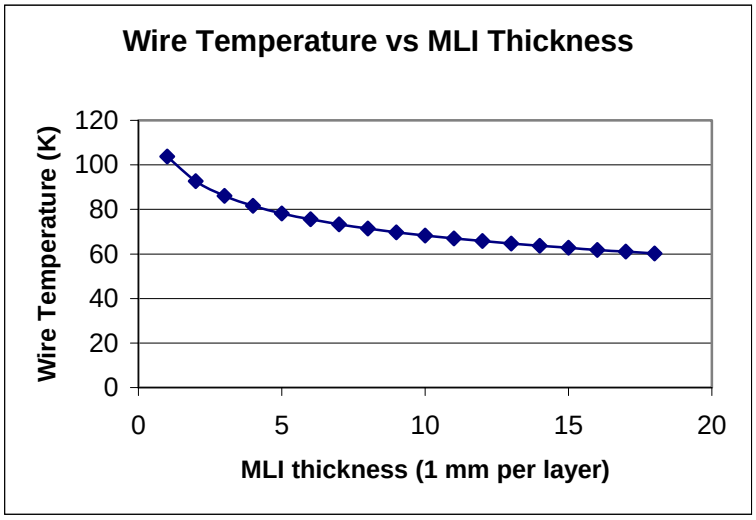

Fig 8: Calculated Wire Temperature

A small peak in the current to coil mass ratio (Fig 9), and payload carrying ability (not shown) is calculated for a 20 km radius operational magsail with an 18 mm thick MLI covering.

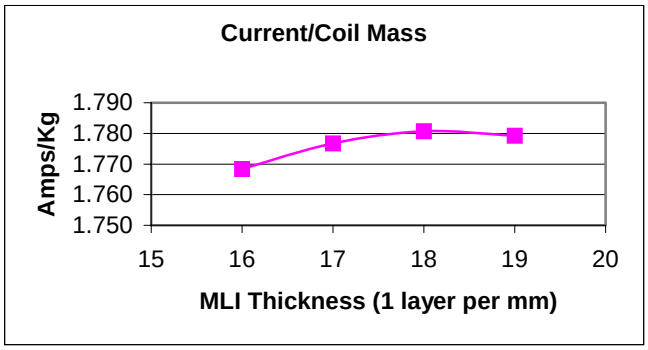

Fig 9: Current to Coil Mass ratio

Additional Limitations, Concerns and Comments:

1) MLI blanket performance:

Wire temperature is very sensitive to MLI blanket and coating performance. In this design, MLI heat transport, which is primarily radiative, is modeled using an effective conduction factor k. The Ag-Teflon coating chosen, is commonly used on MLI, and has much better mechanical characteristics (less brittle) than higher performing Ag-Quartz. These blankets typically have a density of 154 kg /m^3 .[39]

2) Thermal control surfaces:

This design uses a Silver-Teflon solar absorptivity of 0.241 (End of Life value) and an emissivity of 0.66. The White-Epoxy paint emissivity is 0.924.

The MLI blanket is wider than strictly necessary to provide a +/- 10 degrees pointing margin. Using wider MLI could increase this margin. If the superconducting wire and MLI becomes misaligned by more than 10 degrees, it will become illuminated and heat up, causing allowable current in the magsail to drop, possibly leading to a loss of superconductivity

3) Temperature gradients:

In this analysis, a negligible temperature difference, delta T, across the superconducting wire coil was assumed. This approximation will be most applicable for early superconducting wires, which have superconducting filaments in relatively massive metal matrices. More advanced superconducting wire coils may have larger delta T's, across them, but may be able to compensate by using better thermal control coatings and structures. Future wires may also be able to operate at higher temperatures.

4) Cable strength:

Future designs could use filaments internally for strengthening as long as they do not significantly decrease heat flow to radiating surfaces, but were not found necessary in these designs.

Primary Power Trade Study:

Introduction:

The primary power subsystem supplies power for the spacecraft's systems, including the superconducting coil, and control and communication functions.

It is assumed that the biggest use of power will be energizing the magsail coil and that other systems will use secondary power during that time, though primary power can be tapped at the expense of a longer coil charging time.

To obtain the lowest primary power subsystem mass, and thus the highest acceleration/highest payload capacity, it is desirable to have a primary power subsystem with the:

- **highest power density** possible.
- needed **range in power output**
- needed **range in distance** from the Sun
- as much **heritage** as possible.

Once the magsail's payload mass and coil performance are determined, the primary power subsystem main drivers are**:**

- the rate at which the main coil is energized
- distance from the Sun.

In these designs 24 hours has been chosen as a reasonable charge/discharge time, to allow the magsail to travel from Earth Heliocentric Orbit. More advanced designs could use a shorter 30 minute charge time to escape from Earth orbit, via orbit pumping against the geomagnetic poles, and to allow quicker capture at other planets.[14]

The energy (in Joules) ending up in the coils = ½ LI^2 = ½ B A I . (Where L= inductance, B= magnetic field strength in Tesla, A= total area enclosed by coils in m^2 = enclosed area of one coil times # of coils, I = total current in loop in Amps, and $B=B_m = \mu I/2 R_m$ (The B at the center of the loop)

The solar array power requirement includes a multiplier of 1.25 for power conversion loss, 1.4 for End-of-Life-Loss and 2.3 for solar power systems to adjust for the reduced light intensity at Mars. The total multiplier is 4.1. The magsail demonstrator would stay near 1 AU and would therefore have a multiplier of 1.68.

Much beyond Mars, nuclear sources would be needed to charge the magsail. Nuclear power requirements include a multiplier of 1.25 for power conversion loss, 1.4 for End-of life loss, and 1.2 for margin. The total multiplier is 2.1.

Power Densities:

A power density of 50 W/kg is used for present solar arrays. The ultimate performance of solar arrays is assumed to be double the 1998 prototype value of 130 W/ kg.

For outer solar system use, current state-of-the-art power densities, from Cassini, are 5 W/kg. However, the Advanced Radioisotope Power System (ARPS) with 7 W/kg should become available in a few years and an even better AMTEC radioisotope system could attain 12.3 W/kg in a 5-10 yr. time frame. Nuclear reactors may become favorable for very large magsails with increased power demands

Table 5: Primary Power System: [40]

	Power Range (kW)	**Specific Power range (W/kg)**	**Assumed Near-Term Specific Power (W/kg), at 1AU**
Radioisotope	.2-10	5-10	5 [a]
Nuclear Reactor	25-100	15-22	18.5
Photovoltaic (1AU)	.2-25	36-100 [b]	50
Solar Thermal (1AU)	1-300	9-15	12

[a] *State-of-the-art for Cassini* [41]

[b] *Specific power densities have been reported up to 130 W/kg for advanced solar arrays*[42]

Table 6: Power Density at 1 AU

Time	Distance (AU)	System	Power Density (W/kg)
Present	0-3.5	Solar	50
Present	Any	RTG-Cassini [41]	5.09
5– 10 yr.	0-3.5	Advanced Photovoltaic Solar Array **(Prototype 5/7/98)**	130
5 – 10 yr.	Any	RTG-ARPS **(under development, due late 2000)** [41,43]	7.00
5 – 10 yr.	Any	RTG-DIPS **(under development 1989)** [2]	7.5
5 – 10 yr.	Any	Radioisotope AMTEC (Alkali-Metal Electric Conversion) proposed Pluto-Express flyby [44]	12.3
Ultimate	0 –3.5	Solar	260 ?
Ultimate	3.5 +	RTG /Other	?

Conclusion:

Despite losing efficiency with distance, photovoltaics are competitive with RTG's in the inner solar system. For outer solar system use, nuclear power sources are the best (and only) choice.

Current Injection:

Configuration:

The current injection system consists of a solar (or AMTEC) power source, power supply lines, and the power controllers. For redundancy, and symmetric mass distribution, three separate sets of current injection systems could be used, each with the capacity to handle the full current, and supply one-third of the power. Each system would have a "disengaged" default setting to keep the magsail loop circuit closed in the case of injector malfunction or inactivity.

In order to reduce the mass of power transfer lines, the current injection systems would placed under the solar arrays, which in turn would be placed on the rim of the magsail next to the magsail loop. This would have the added benefit of shading the power control and injection equipment and part of the cable.

Operation:

In each injection system, the current will flow from the power source(s) through power lines into the controller. The power will be fed through all but a few centimeters of the magsail loop, nearly completing an entire circuit. The current is then shunted to back into the controller, which continually adds energy and completes the circuit. The entire loop will act as a large inductor.

The superconducting wire will be composed of many smaller filaments to reduce the total current needed. For instance if the Operational magsail uses a cable 2.35 x 2.35 mm comprised of 529 individual filaments, each about 0.1 mm x 0.1 mm, the current needed would drop by a factor of 529, as compared to a single wire. Each filament would include a thin electrical insulation coating, whose mass and impact on overall current density is assumed negligible,

For the full sized magsails in this report, the loop self-inductance, L

$= \phi_{B\ coil}/I = n\ \phi_{B\ one\ loop}\ /I$
$= n^2(\Pi R^2 B)/I$
$= \mu_0 \Pi R n^2/2$

for

$R= R_m = 2 \times 10^4$ m,
$B=B_m= \mu_0 nI/2R$
$n=\#_{coils,}$ total current = nI ,
current in filament = I

$dI/dt=-(EMF/L)$.

For a 20 km radius magsail using a multistranded wire with L 1.11 x 10^4 H, a constant EMF of 3.86 Volts will increase the current in a magsail loop by 3.49 x 10^{-4} A/s. After 24 hours, the power flowing into the circuit will rise to 151.9 W, and the magsail loop would reach its final current of 1.596 x 10^4 A (with 30.17 A in each strand).

If power margins are gained by increasing voltages, the Solar magsail needs 15.82 V, 622.8 W, the AMTEC magsail needs 8.10 V , 319.0 W.

The magsail Demonstrator, (L=20.00) would need 91.9 seconds to charge up to 4.60 A/filament at 1.0 V and 4.60 W. (This assumes a voltage below 1 V would be impractical) Adding margin, 1.68 V and 7.73 W would be needed

During charge-up the entire current will be flowing through the magsail and power controller. In order to keep current from falling after charge-up, a superconducting switch will close to complete to magsail circuit and a switch to the power controller will be opened. If any minor losses still exist, they can be detected by monitoring the magsail's magnetic field and topping off the current as needed. (This will probably be necessary for early BSCCO based demonstrators which will experience current decay due to flux creep.)

To charge up the 20 km solar powered Operational magsail in only 30 minutes, in Earth orbit rather than heliocentric orbit, would require a much larger power source, resulting in lower payload capacity. The 20 km solar magsail would require 759.3 V, 22.91 kW, with margin. The 20 km AMTEC magsail would require 3.89 V, 1.17 kW, with margin.

Connection to Power System:

Low capacity power or control lines could be threaded from the solar arrays and power controller through the tethers to the central hub if desired, but should not be necessary.

The mass budget of the power control and distribution subsystems (excluding power supply) is included in the mass budget of the central hub/support equipment.

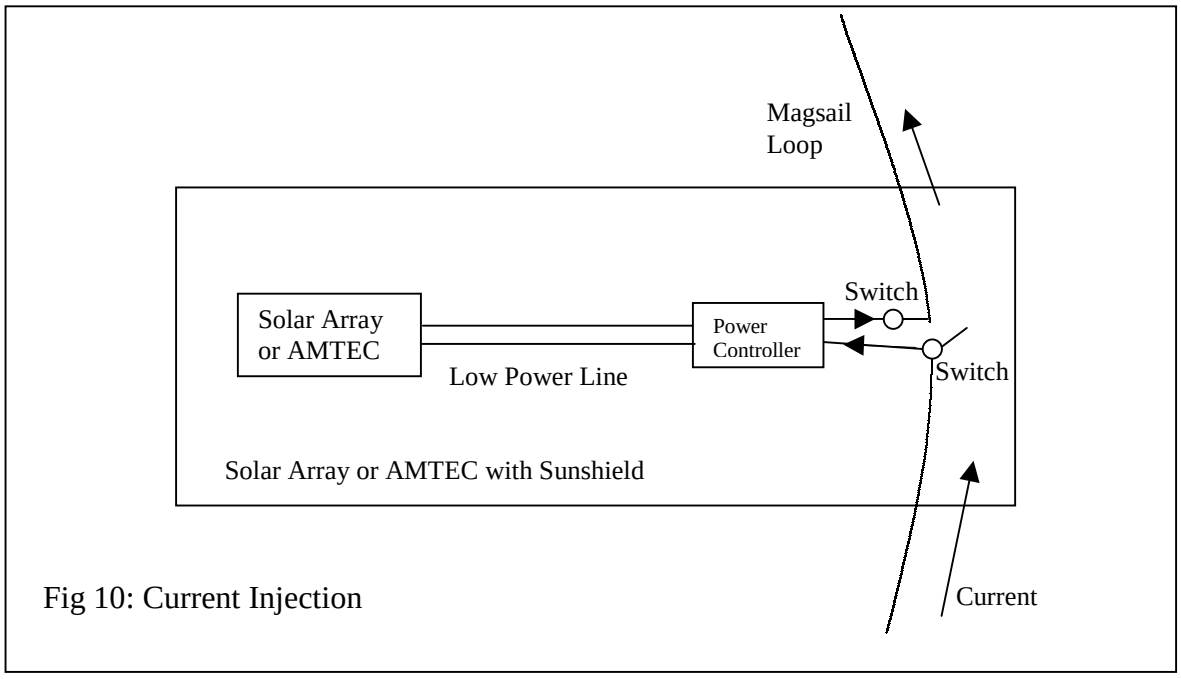

Fig 10: Current Injection

Shroud Lines:

Shroud lines are needed to attach the payload and control systems to the magsail coil. The shroud lines do not take up any stress from the current loop. Magsail accelerations are very small, so the worst stress on the shroud lines will be from shifting the magsail's center of mass to control attitude. As an example, to move the magsail center-of-mass by 2.0 km in an hour one (10 % of the radius), the current loop would have to move an average of 0.556 m/s. By accelerating to a peak velocity halfway before slowing down, a maximum kinetic energy of 6,697 J would be attained in moving a 10,849 kg magsail payload. This corresponds to an average power requirement of 3.72 W. The required acceleration would only be 6.17×10^{-4} m/s^2, (V_{max}/30 minutes), corresponding to a force of 6.70 N (1.51 lbf)

Three strands of Spectra® fibers from Allied Signal would more than fill the tether requirements for strength. Spectra is one of the lightest, strongest, and UV resistant commercial aerospace fibers available. [45] However considering the low mass of these fibers relative to the mass of the rest of the magsail, it would be prudent to use larger tethers designed to survive micro-meteoroid strikes over the period of many decades. Tethers Unlimited already makes ultra long life tethers for space applications. These "Hoytethers" are made from Spectra 2000 and have anticipated lifetimes of several decades. According to Dr. Robert Hoyt, a tether flown on the ProSeds mission had a mass of only 1,820 g for a 10,300 m length. This tether had a wound volume of 3,640 cm^3, and a breaking strength of 200 N. While tethers could be made smaller than this, there are limitations due to the size of the secondary, knitting, lines.[46]

In the magsail designs, three scaled up ProSeds tethers can be used for the shroud lines. An 24 km shroud line would have a mass of 4.24 kg, a breaking strength of 200 N, and a wound volume of 8,481 cm^3.

If the superconducting wire can be cooled to a superconducting state before deployment, the shroud lines could be deployed by charging up the magsail. After releasing the shroud lines, the magnetic fields generated would cause the magsail to inflate. As the shroud lines unwound off their spools, the magsail line spools, housed with the solar arrays and current injection systems, would move outwards. The magsail line spools, containing the magsail wire and insulation, would move farther away from each other and unreel. For deployment the charge time will probably be lengthened to minimize stresses on the current loop, but remain shorter than the deployment time.

Deployment of Magsails in a Non-Superconducting State via Magnetic Fields

Of all the engineering issues associated with magsail technology examined in the study, the most critical was found to be that of deployment. (In contrast, power systems needed to put the current in the magsail within 24 hours, and weight shifting shroud systems used to control magsail orientation were found to be very modest, and well within the range of existing technology.)

The problem is this: One could use the superconducting current to create I X B forces in the cable, and the resulting hoop stress would deploy the loop into a circle within a time much shorter than that needed to insert the current (i.e. << 24 hours). So far, so good. But unless the magsail is operating in an environment where the ambient temperature allows it to be superconducting without shielding (i.e. either the magsail is in interstellar space, or if at 1 AU, room-temperature superconductors are available), the magsail will not be superconducting until after it is deployed and properly oriented. So in general, super conducting current will not be available to deploy the magsail.

However, the magsail cable is predominantly composed of silver, which is an excellent normal conductor. Depending on the coil geometry and the size of the power source available, this can carry a current that may be sufficient to deploy the cable. We can calculate a characteristic time for the deployment as follows.

Since elementary dynamics gives the distance traveled by an accelerating object as $R=0.5At^2$, we have the characteristic time for deployment is;

$$T = (2R/A)^{0.5} \qquad (11)$$

Where A, the characteristic acceleration is given by

$$A = IB2\pi R/M = \mu\pi I^2/M \qquad (12)$$

Where I is the total current and M is the mass of the cable. For slow inflations, inductive resistance is negligible, so the current is given by;

$$I^2 = Pa/2\pi\rho R \qquad (13)$$

Where P is the power, a is the wire cross sectional area, and ρ is the resistivity.

Combining expressions (11), (12) and (13), we obtain;

$$T = 2R\,(M\rho/\mu Pa)^{0.5} \qquad (14)$$

Using equation (9) we calculate that the Operational magsail, if equipped with a 10 kWe power supply, would be able to deploy itself in 1.95×10^6 s, or 22.57 days. The smaller

Demonstrator magsail, if equipped with a 100 W power supply, would be able to deploy itself in 30,100 s, or 8.36 hours.

This calculation ignores the slow down of deployment due to viscous resistance from the cable, and also the acceleration of deployment caused by the fact that initially the uncoiled cable has its segments very close together, thus amplifying the magnetic hoop force. These two considerations cancel each other to some extent. But conceding the approximate nature of the calculation, it can be seen that the use of the resistive metal substrate to carry a normal current is probably feasible for small magsails like the demonstrator, but will become impractical as the magsail increases with size.

If the magsail dimensions are such that normal current deployment become impractical, alternative methods of deployment, such as inflatable booms or spacecraft rotation will need to be employed.

How a magsail deployment system might pay out its cable is depicted in Fig. 11.

The practical limits of the use of normal current to deploy the magsail thus need to be defined more precisely. This can be done by measuring the mechanical properties of actual magsail cable, and then performing detailed finite-element dynamic simulations of the deployment process. Such an investigation is proposed as part of the Phase II program.

Fig 11: Magsail Deployment Diagrams

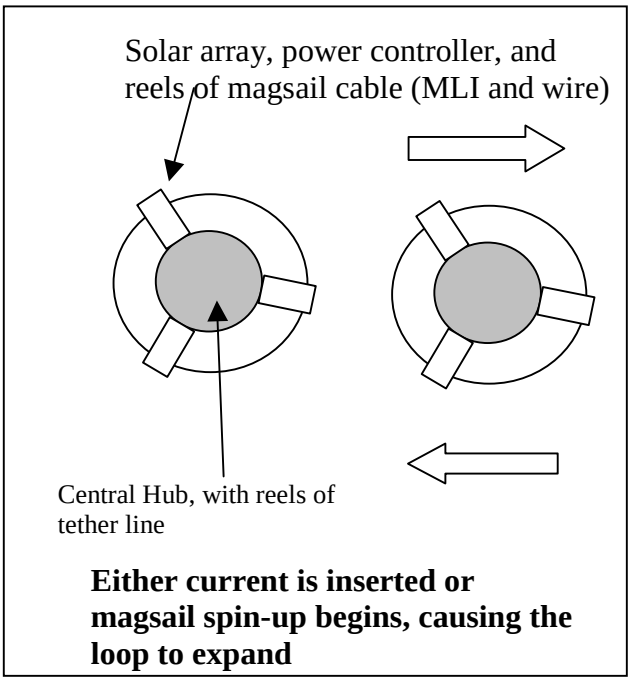

Either current is inserted or magsail spin-up begins, causing the loop to expand

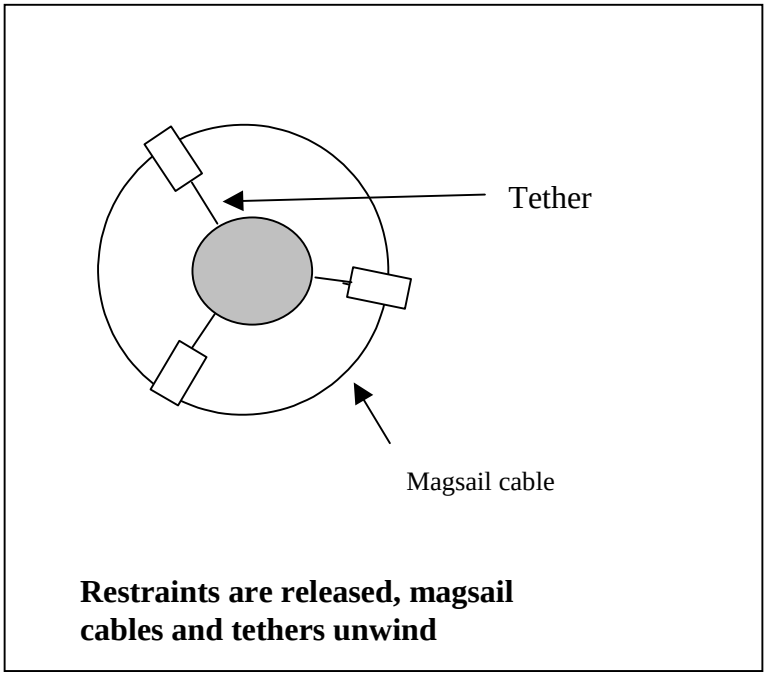

Restraints are released, magsail cables and tethers unwind

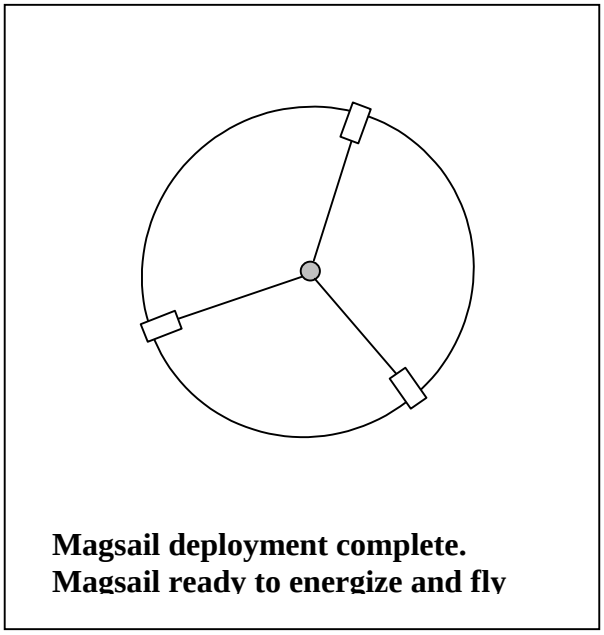

Magsail deployment complete. Magsail ready to energize and fly

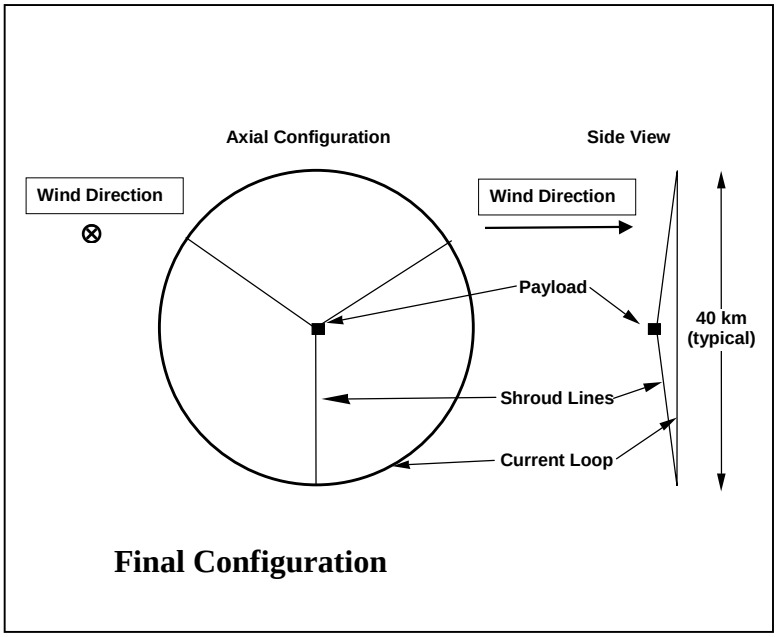

Final Configuration

Shroud line and Magsail line spools:

Each of the three shroud line spool will be attached near a rim mounted solar array. For the full sized magsails, each shroud line spool needs to contain 0.006361 m^3 of shroud line and any additional (optional) power or control cable leading to the hub. Assumming no extra power or control cable is used, and assuming spool inner diameter, outer radius, and width are all the same, each shroud line spool would have a volume, $V = 3 \pi R_i^3$. Each of the shroud line spools would measure 9.65 cm wide with an 9.65 cm inner radius and a 19.31 cm outer radius.

Similarily, each of the six full-sized magsail cable spools (magsail wire and MLI) would have an inner radius and width of 0.74 m, an outer radius of 1.47 m, and volume 3.75 m^3

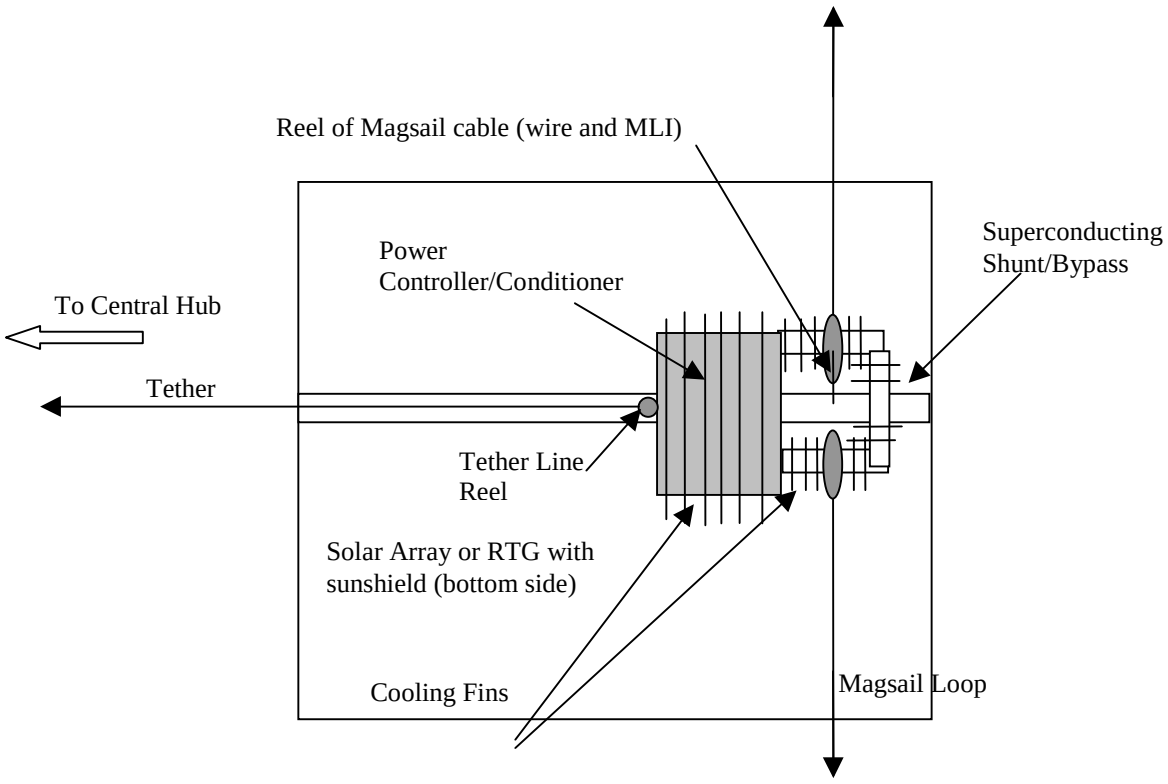

Fig 12: Magsail Connection Node: including power supply, power control, power injection, coil deployment spools, and tether attachment node.

Magsail Designs

Introduction:

Both a 200 m radius – Demonstrator and a 20 km radius - near-term "Operational" magsail were designed. Their central Magnetic Fields, B_m are respectively 32.5 and 5.01 x 10^{-7} T. Since both of these are much greater than the 5.18 x 10^{-8} T needed to block the solar wind, they should avoid solar wind "punch through" in all but extreme circumstances. The required superconductor Engineering Critical Current Density, J_e for the demo is already attainable in 10 cm lengths of commercial BSCCO wire, and in 1 m lengths of YBCO thick film coated conductors. The Operational magsail J_e is not yet available, but corresponds to a very near-term (2005) extrapolation of the technology.

The acceleration of the magsail coil, not taking into account other masses has been calculated as:

$$D/M = 0.59 (\mu\rho^2 V^4 R_m/I)^{1/3}(J/\rho_m)$$

When this is divided by the weight ratio (total mass of the loaded spacecraft divided by the coil mass) it yields the net acceleration. Also of interest is the Payload Ratio which is the Payload mass divided by the unloaded magsail spacecraft mass.

The characteristics of each of these designs is given in Tables 7,8, and 9..

Temperature and J_e:

The baseline magsail designs are optimized to operate in heliocentric space between Earth and Mars at a maximum temperature. However, when the magsails are farther than 1 AU from the Sun, temperatures will drop, allowing payloads to be moved more rapidly, as long as the coils are charged/discharged an additional amount at the appropriate times. This is analyzed later in more detail under orbit pumping and maximizing current.

In each design, the magsail coil has a small wire with a square cross-section, shaded by a thick wedged shaped MLI blanket.

The coils will maintain their operational temperature even after the Ag-Teflon coatings have aged, provided the magsails remain aligned to the Sun within 10 degrees of arc.

Assuming a negligible thermal gradient across the wire, the magsail coil temperature will stay cool through radiative means.

The engineering critical current density for state-of-the-art BSCCO wire used in the demonstrator is estimated as 5.82 x 10^8 A/m^2 at 63.9K, approximately 2.0 times its value at 77 K value. It is assumed that the more advanced superconducting wires (YBCO, etc.) will have a higher overall J_e , but exhibit a similar trend in J_e vs. T as in Fig 13.

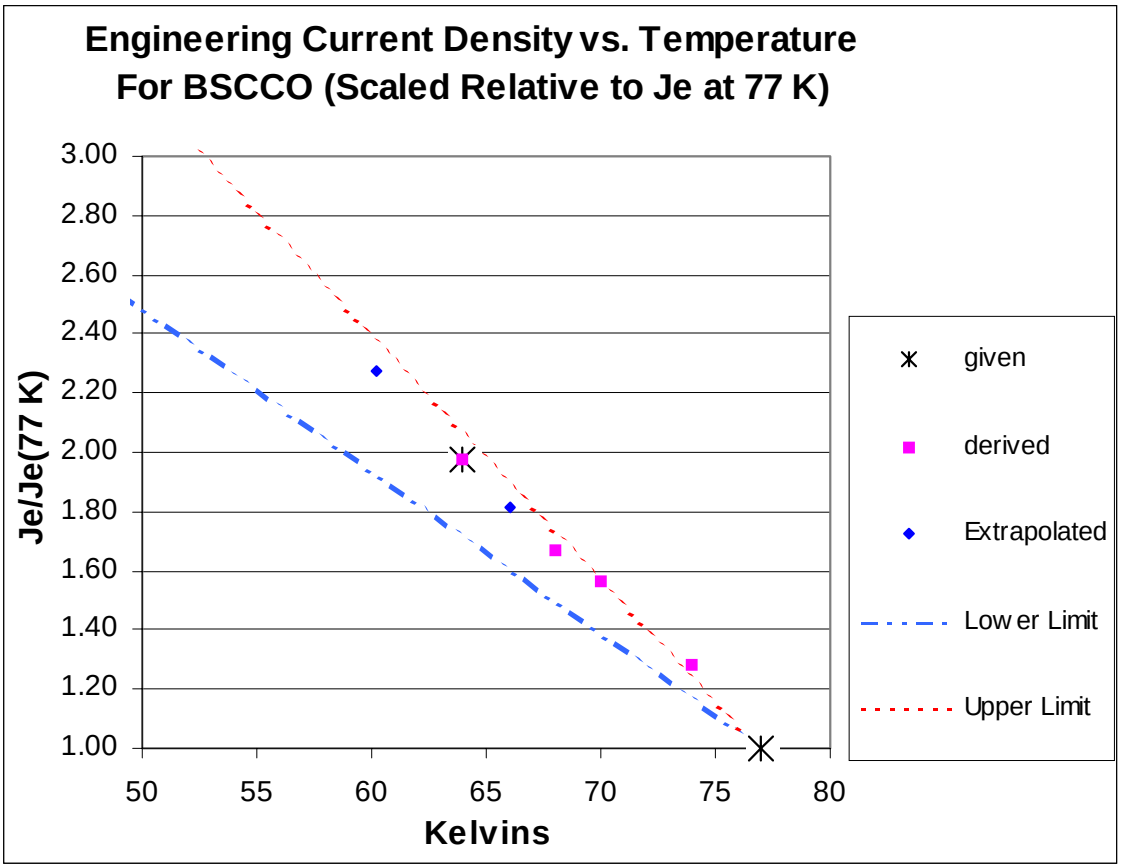

Fig 13: Estimated Je vs T for BSCCO wire:

Given J_e at 64 K and 77 K, nearby data points were derived by using data on I(T) vs I at 65K [24]. Further data points were extrapolated by using the linear behavior of J_e vs T below 65 K [47]. For example, the J_e at 60.2 K was calculated as 5.23×10^8 A/m^2, 2.27 times its value at 77 K. (This is in line with other derived values, though near the upper limits of J_e given by Larbalesteier, who gives the J_e at 4.2 K as 5 to 7 times its J_e at 77 K.[18]

Wire density:

The BSCCO wire in the demonstrator has a density of about 9 X 10^3 kg/m^3, which is mostly silver. As wires improve, metal content will drop and densities will move closer towards 5.00 X 10^3 kg/m^3, the density of pure copper oxide. It is assumed here that wire density will fall to about 8.00 X 10^3 kg/m^3 in 5-10 years. Because metal in the wire is important for thermal and electrical conductivity, as well being a substrate, 7.00 X 10^3 kg/m^3 has been chosen as a good guess for the ultimate wire density, rather than lower value of 5.00 X 10^3 kg/m^3.

Magsail Demonstrator Designs:

Magsail Demonstrator:

A small demonstrator magsail optimized for a radius of 200 m and a total mass of 100 kg could reach an apoapsis of at least 1.0267 AU, without pumping or other optimization techniques Early in its life, before its Ag-Teflon coatings aged, it would perform better. It would have a 25.7 kg, wire mass, a 10 kg payload, and a 40 kg hub spacecraft with supporting equipment. If its 10 W of power can be efficiently channeled into its coils, it could charge up it coil in less than a minute.

Such a technical demonstrator would be able to develop magsail technology and operational procedures, as well as conduct a large number of science observations on the Sun, Earth, Moon, and multiple Near Earth Objects. There are hundreds of NEO's that cross Earth's orbit, many at a closer distance.[48]

Magsail Demonstrator data is presented in Table 7)

Table 7 Magsail Demonstrator Data:

Coil Characteristics:

Wire:

Coil Temperature:	63.9 K (max)	
Wire density:	9.00×10^3 kg/m^3	
Current density, J_e :	4.56×10^8 A/m^2	
Current per filament:	4.60 A	(225 filaments 0.1 mm x 0.1 mm)
Total Current:	1.03×10^3 A	
Self-Inductance:	20.00 H	
Magnetic Field, B_m:	3.25×10^{-6} T	
Coil Stress:	0.17 Mpa	
Force/Length:	3.36×10^{-3} N/m	(Fully Inflated)
Radial Expan. Accel:	~2.41×10^{-4} m/s^2	(Fully Inflated)

Width:	1.51 mm
Thickness:	1.51 mm
Radius, R_m:	2.00×10^2 m
Mass Coil wire**:**	25.70 kg

MLI:

Avg. allowable tilt:	0 – 10 degrees	
MLI width:	2.04 mm	(min)
MLI width:	6.62 mm	(max)
MLI thickness:	13.0 mm	
MLI density:	154 kg/m^3	
MLI Mass:	9.0 kg	

Coatings:

Ag-Teflon emiss.:	0.790	
Ag-Teflon absorpt:	0.241	(End-of-Life)
White Epoxy emiss.:	0.924	

Thermal Coating Mass: 0.1 kg (assumes density of 9×10^3 kg/m^3 , 1 micron thick)

Environment:

Solar wind density: 8.35×10^{-21} kg/m^3 / AU ^{2} -- at 1AU
Solar Wind Velocity: 5.00×10^5 m/s

Power*:

Coil Energy:	210.9 J	
Elec. Power:	7.73 W	
Voltage:	1.68 V	
Specific Power:	50 W/kg	(solar array)
Solar array radius:	0.114 m	(14 % efficiency)
Solar Panel Mass:	0.115 kg	
Charge time$^+$:	91.1 seconds	
Power margin:	1.68	(for 1.0 V minimum voltage)

* Beginning of Life at 1 AU
$^+$ Assumes negligible flux creep in superconductor

Misc.

Tether Mass:	0.175 kg	
Spacecraft systems:	40 kg	(spacecraft structure, equipment, and central hub)
Margin:	1.2 multiplier	

System Mass:

Coil wire:	25.70 kg
MLI:	9.0 kg
Thermal Coatings:	0.1 kg
Solar Arrays:	0.115 kg
Tethers:	0.175 kg
Spacecraft Systems:	40.0 kg
Margin:	15.0 kg
Payload:	10.0 kg
Total Unloaded Mass:	90.0 kg

Payload: 10.0 kg

Total System: 100.0 kg

Performance:

Magsail Mass:	90.0 kg	(without payload)
Payload:	10.0 kg	
Weight Ratio:	3.90	(Total system mass/ coil mass)
Payload Ratio:	0.111	(cargo mass/ unloaded magsail mass)
Self-Acceleration:	0.000305 m/s^2	
Apoapsis:	1.0267	(At Constant Alpha ,α)

Optimized Operational Magsail Design:

By varying the parameters of R_m, MLI width, and MLI thickness, a solar powered magsail design was optimized for use between Earth orbit and Mars orbit. The magsail's performance is optimized using the highest temperature that it will encounter, at 1AU, though its actual performance can be increased as its temperature drops, farther from the Sun.

The magsail has a mass of 1.084×10^4 kg and can carry 1.096×10^4 kg to 1.5237 AU (Mars orbit). The payload ratio (payload mass/ empty magsail mass) is 1.011.

This magsail has a square wire 2.65 mm thick comprised of 529 filaments each 0.1 x 0.1 mm wide. The wedge shaped MLI blanket has a minimum width of 3.58 mm, a maximum width of 9.93 mm, and a thickness of 18.0 mm. The magsail loop has an radius, R_m, of 20 km and generates a magnetic field, B_m, of 5.01×10^{-7} T in its center.

A radius of 20 km was chosen as a practical value of R_m. At lower values of R_m, the payload-to-magsail mass ratio drops as effects from a decreasing loop area grow faster than the effects from the increasing magnetic field strength. At lower values of MLI thickness, the payload ratio drops as the effects of increasing temperature rise faster than mass reduction effects. At higher values of MLI thickness, the payload ratio drops as the effects of increasing mass effects overtakes the gains made from a lower temperature. MLI width is scaled with wire size to maintain pointing margin. Thicker wire results in slight decreases in payload ratios and thinner wire decreases B_m.

The design data for this operational magsail is presented in Table 8.

Table 8. Operational Magsail Data:

Coil Characteristics:

Wire:

Coil Temperature:	60.2 K (max)	
Wire density:	8.00×10^3 kg/m^3	
Current density, J_e :	2.27×10^9 A/m^2	
Current per filament:	30.17 A	(529 filaments 0.1 mm x 0.1 mm)
Total Current:	1.60×10^4 A	
Self-Inductance:	1.105×10^4 H	
Magnetic Field, B_m:	5.01×10^{-7} T	
Coil Stress:	1.51 Mpa	
Force/Length:	8.00×10^{-3} N/m	(Fully Inflated)
Radial Expan. Accel:	9.27×10^{-2} m/s^2	(Fully Inflated)

Width:	2.65 mm
Thickness:	2.65 mm
Radius, R_m:	2.00×10^4 m
Mass Coil wire**:**	7.06×10^3 kg

MLI:

Avg. allowable tilt:	0 – 10 degrees
MLI width:	3.58 mm (min)
MLI width:	9.93 mm (max)
MLI thickness:	18.0 mm
MLI density:	154 kg/m^3
MLI Mass:	1.893×10^3 kg

Coatings:

Ag-Teflon emiss.:	0.790
Ag-Teflon absorpt:	0.241 (End-of-Life)
White Epoxy emiss.:	0.924

Thermal Coating Mass: 9.2 kg (assumes density of 9×10^3 kg/m^3 , 1 micron thick)

Environment:

Solar wind density: 8.35×10^{-21} kg/m^3 / AU ^{2} -- at 1AU
Solar Wind Velocity: 5.00×10^5 m/s

Power*:

Coil Energy:	5.027×10^6 J	
Elec. Power:	622.8 W	
Voltage:	15.82 V	
Specific Power:	50 W/kg	(solar array)
Solar array radius:	1.02 m	(14 % efficiency)
Solar Panel Mass:	12.46 kg	
Charge time:	24 hrs.	(at 3.86 V, 151.9 W)
Power margin:	4.1	

(*Beginning of Life at 1 AU)

Misc.

Tether Mass:	12.72 kg
Spacecraft systems:	50 kg (spacecraft structure, equipment, and central hub)
Margin:	1.2 multiplier

System Mass:

Coil wire:	7.060×10^3 kg
MLI:	1.893×10^3 kg
Thermal Coatings:	9.20 kg
Solar Arrays:	1.246×10^1 kg
Tethers:	1.27×10^1 kg
Spacecraft Systems:	5.00×10^1 kg
Margin:	1.807×10^3 kg
Total Unloaded Mass:	1.084×10^4 kg
Payload:	1.096×10^4 kg
Total System:	2.180×10^4 kg

Performance:

Magsail Mass:	1.084×10^4 kg (without payload)
Payload:	**1.096×10^4 kg (Mars)**
Weight Ratio:	3.09 (Mars) -- *(Total system mass/total coil mass)*
Payload Ratio:	1.011 (Mars) -- (cargo mass/ unloaded magsail mass)
Self-Acceleration:	3.185×10^{-3} m/s^2
Apoapsis:	1.5237 AU (At Constant Alpha ,α)

Table 9. Comparison of Magsail Designs:

	Demonstrator	Operational
Wire:		
Coil Temperature:	63.9 K (max)	60.2 K (max)
Current density, J_e :	4.56×10^8 A/m ^{2}	2.27×10^9 A/m ^{2}
Current per .01 sqmm fil.	4.60 A (225 filaments)	30.17 A (529 filaments)
Magnetic Field, B_m:	3.25×10^{-6} T	5.01×10^{-7} T
Radius, R_m:	200 m	20 km
MLI:		
MLI width: (min - max)	2.04 mm - 6.62 mm	3.58 mm - 9.93 mm
MLI thickness:	13.0 mm	18 mm
Performance:		
Coil Mass:	25.70 kg	7060 kg
Other S/C Mass: (w/o payld)	64.3 kg	3780 kg)
Payload:	10.0 kg	10,960 kg (to Mars)
Weight Ratio:	3.90	3.09 (to Mars)
Payload Ratio:	0.111	1.011 (to Mars)
Self-Acceleration:	0.000305 m/s^2	3.185×10^{-3} m/s^2
Apoapsis:(@ Constant α)	1.027 AU	1.524 AU

Ultimate Magsail Performance:

Magsails could eventually explore the outer solar system and more easily transport cargo to the inner planets as wire performance improves. On the basis of applicable data it appears that the J_e of superconducting wires could ultimately rise above 2.27×10^{11} A/m^2 at 60.2 K, with a density below 7×10^3 kg/m^3. This could, when coupled with likely advances in power supplies, structures, insulation, etc., lead to 20 km radius magsails AMTEC powered magsail with very high payload ratios ranging from Mercury and Mars to 1,000 AU and beyond. The performance of such a system is displayed in Table 10. An AMTEC power supply is assumed.

Table 10: Ultimate Magsail: Payload Vs Distance
(Unloaded mass = 9.801×10^3 kg, R_m=20 km)

Destination	**Distance**	**Payload from Earth**	**Payload ratio**
	(AU)	(kg)	
Mars	1.524	4.600×10^5	46.9269
Jupiter	5.203	1.901×10^5	19.3928
Saturn	9.539	1.706×10^5	17.4026
Uranus	19.191	1.605×10^5	16.3788
Neptune	30.061	1.572×10^5	16.0401
Pluto	39.469	1.559×10^5	15.9008
Kuiper Belt	1,000	1.518×10^5	15.4897
Ort Cloud	10,000	1.517×10^5	15.4749

Magsail Orbit Simulations

The analytic magsail theory developed by the Principal Investigator in reference 2 allows the calculation of zero-lift magsail orbits under conditions of constant alpha. These orbits can be calculated analytically, because they are quasi-Keplerian, with the key distinction being that the spacecraft's orbit corresponds to that of one traveling around a Sun of apparently reduced mass. However, while simple to calculate, such constant alpha orbits do not represent the full capability of a magsail spacecraft. To calculate more complex orbits which more fully demonstrate the magsail's capability, computer simulations were performed. The trajectory types examined included;

1) Constant alpha. In these orbits, the magsail current is reduced as the spacecraft moves away from the sun, so as to keep the apparent solar gravity on the spacecraft constant. As mentioned above, such orbits can be calculated analytically. The primary purpose in repeating the calculation with the computer code was to validate the code.

2) Constant current. In these orbits, the current initially put in the magsail is kept constant, which therefore causes alpha (the Sun's apparent mass) to decrease slightly as the spacecraft increases its distance. Simulations showed that such trajectories offer only very modest improvements over constant alpha trajectories.

3) Maximum current. In these orbits, the magsail current is increased as the spacecraft moves away from the Sun. This is possible, because as the spacecraft increases its distance from the Sun, the superconducting wire becomes colder, and its current carrying capacity increases. In some cases, this maximum current mode offers a significant increase in magsail performance verses the constant alpha baseline.

4) Pumped orbits. In these instance, maximum current is maintained in the magsail while it is moving away from the Sun, but then the current is turned off while the spacecraft descends towards the Sun. Such a system conserves angular momentum. But its energy increases, as the apparent solar gravity felt by the spacecraft when it is falling is greater than that it must work against when it is climbing. As a result, this mission mode offers drastic expansion of magsail capability compared to that predicted by constant alpha trajectories.

The following Orbit plots, (Fig. 14,15,16) show three different cases for the 'Operational' magsail.

In Fig 14, the simple case of a constant Alpha, effective reduction in the Sun's gravity due to the magsail's thrust, is shown. This is the case for which all previous calculations have been based.

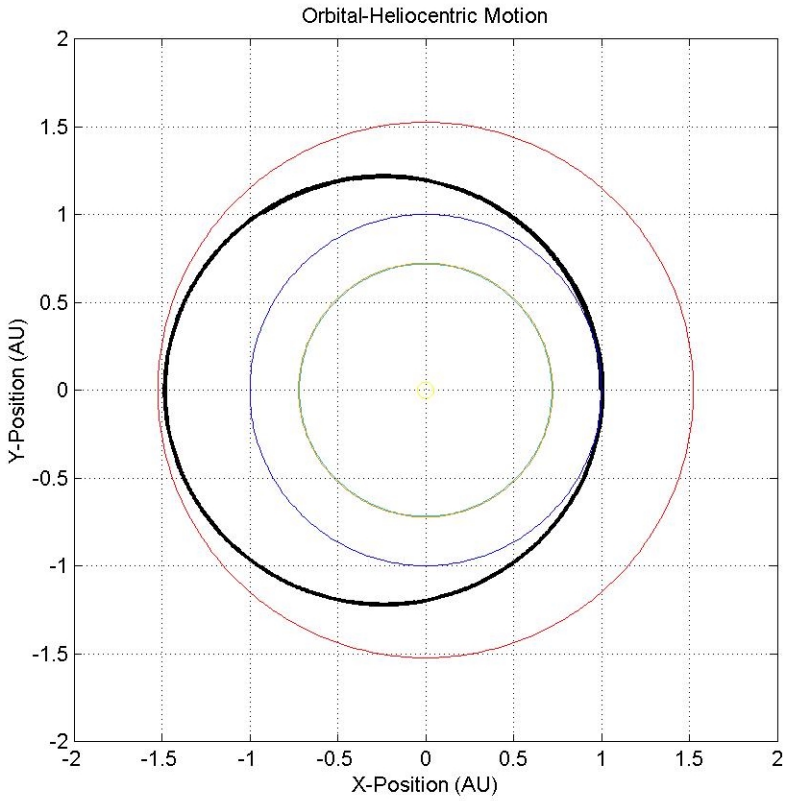

Fig 14: Orbit for Constant Alpha, payload ratio = 1.0
Orbits of Venus, Earth, and Mars also shown

For each of these cases, the orbit was iteratively calculated by computer code. Several refinements were made to previous approximations. The solar wind speed was reduced to 480 m/s = $(.5(V_{wind\ MAX}{}^4 + V_{wind\ MIN}{}^4))^{1/4}$, where V_{wind} ranged from 350 m/s to 550 m/s, to better approximate the solar wind's effective average speed. In addition the relative motion of the magsail, the changing temperatures, and solar wind densities were accounted for.

In the following analysis we consider a magsails with a 'baseline' engineering critical current density of 2.30×10^8 A/m^2 - demonstrator magsail, 10^9 A/m^2 – 'Operational' magsail, and 10^{10} A/m^2 – advanced magsail. The actual J_e 's are assumed to be higher at their lower operating temperatures, following the same linear (J_e vs T) relationship as present commercial wires. The ratio of payload mass to unloaded magsail mass, the payload ratio, is assumed to be 1.0. Though much larger payload masses could be moved to farther distances with increased travel time, eventually the trade-off of a longer flight time will have to be weighed against delaying a mission to develop the technology for a faster magsail.

After the above refinements, the resulting apoapsis for the constant alpha case of the operation magsail with a payload ratio of 1.0, is reduced to 1.484 AU.

In **Fig 15,** and **Fig 16**, the maximum allowable current is passed through the magsail. The current level is increased as the magsail moves away from the Sun and the temperature drops, increasing the critical current density. As a result its first apoapsis reaches just past Mars to 1.6143 AU. It also experiences significant 'precession' and subsequent orbit circularization.

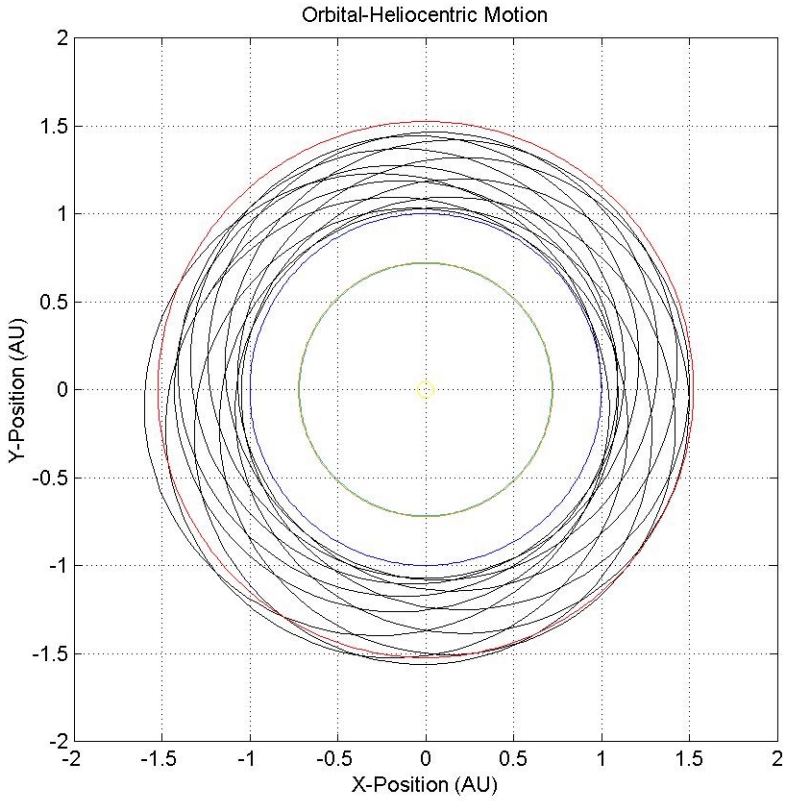

Fig 15: Orbit for Maximum Current, payload ratio = 1.0
Orbits of Venus, Earth, and Mars also shown.

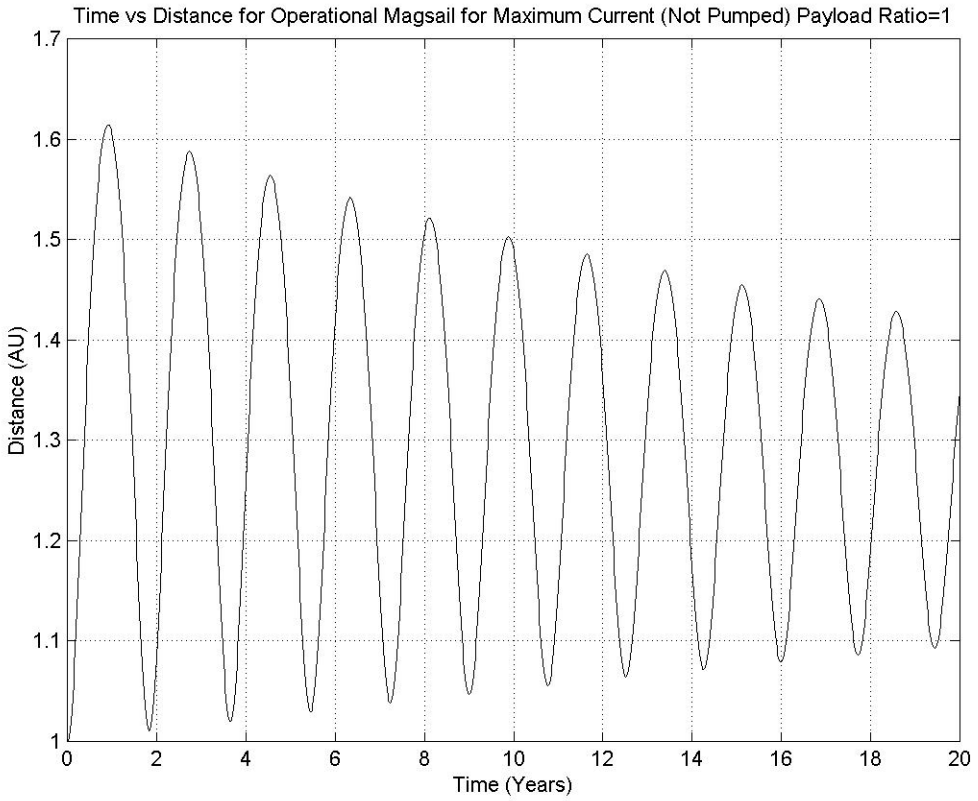

Fig 16: Distance vs Time for Maximum Current, not pumped, payload ratio=1

We now turn to an examination of the strategy we term 'pumping' in which the magsail is only turned one while the spacecraft is moving away from the Sun but is turned off when it is falling towards the Sun. Since, in this case, the Sun's acceleration, "effective Sun" is greater than when falling than rising, such a system is non-conservative, and the energy of the spacecraft can be increased with each orbit.

If a 'pure' orbit pumping approach is used, turning on the magsail only when outbound from the Sun, the Magsail's orbit will steadily increase in size until it reaches solar escape velocity. If the maximum allowable current is used along with pumping, a magsail with a payload ratio of 1.0 could reach Mars in about 7.7 months (~ 0.64 sidereal years). It would then loop back toward the Sun, reaching a periapsis of 0.7248 AU and boost its orbit. On its next orbit it will cross Mars' and Jupiter's orbit to reach an aphelion of 6 AU, before its final solar approach. After its final solar approach, at 0.5457 AU, it would escape the solar system. Sailing past Jupiter one last time, ~10 years after its initial launch. (Fig 17, Fig 18)

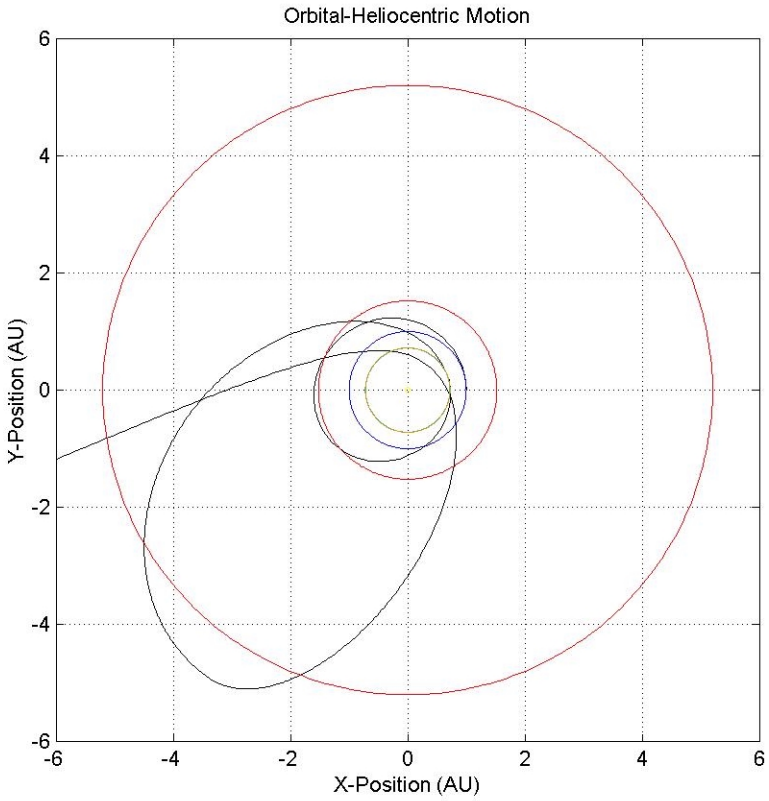

Fig 17: Orbit for Maximum Current, pumped, payload ratio=1
Orbits for Venus, Earth, Mars, and Jupiter also shown.

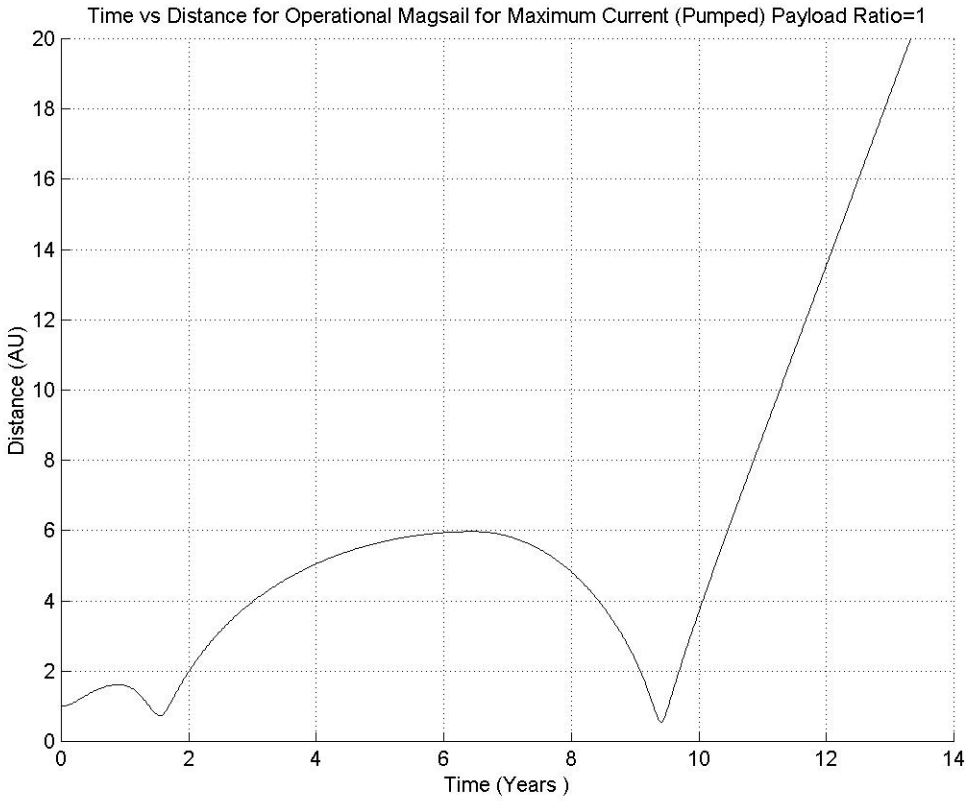

Fig 18: Time vs Distance for Maximum Current, pumped, payload ratio=1

A modified orbit pumping approach can be used to alter performance even further. For instance, the magsail can be turned off when outbound from the Sun and at a distance greater than 1.5 AU, until it perihelion reaches below 0.56 AU, (As well as being turned off during its normal inbound flight.) The magsail would then stay closer to the Sun longer and end up leaving the solar system about 2 years earlier than before, but it would leave at a slightly lower speed.(Fig 19, Fig 20) In other cases both a gain in final speed and a shorter time until escape may be possible.

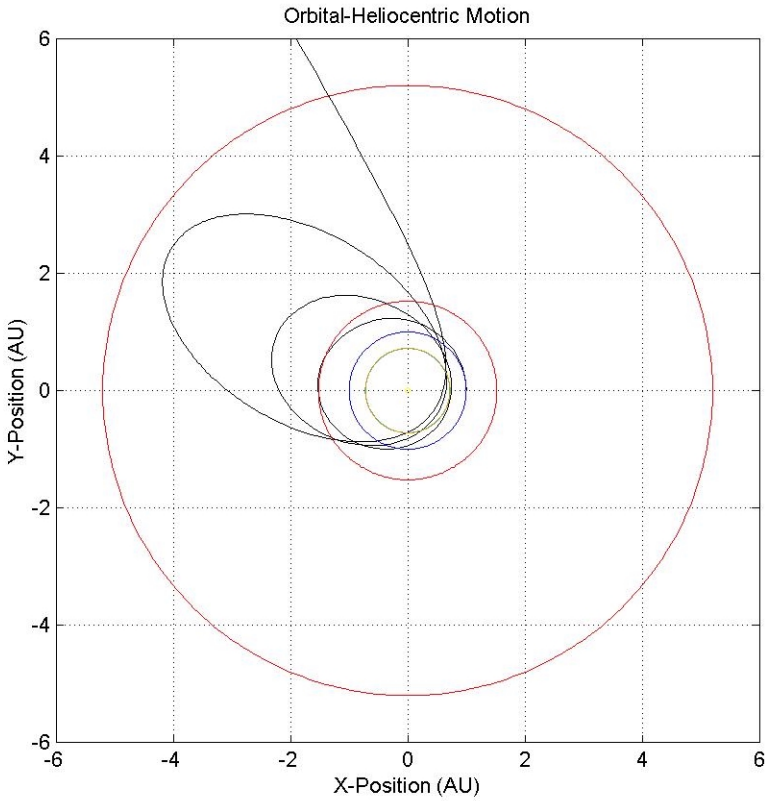

Fig 19: Orbit for Maximum Current, Modified pumping, payload ratio=1
Orbits for Venus, Earth, Mars, and Jupiter also shown. (Magsail turned off on sunward orbit and also turned off at farther than 1.5 AU , until perihelion has decreased below 0.56 AU.)

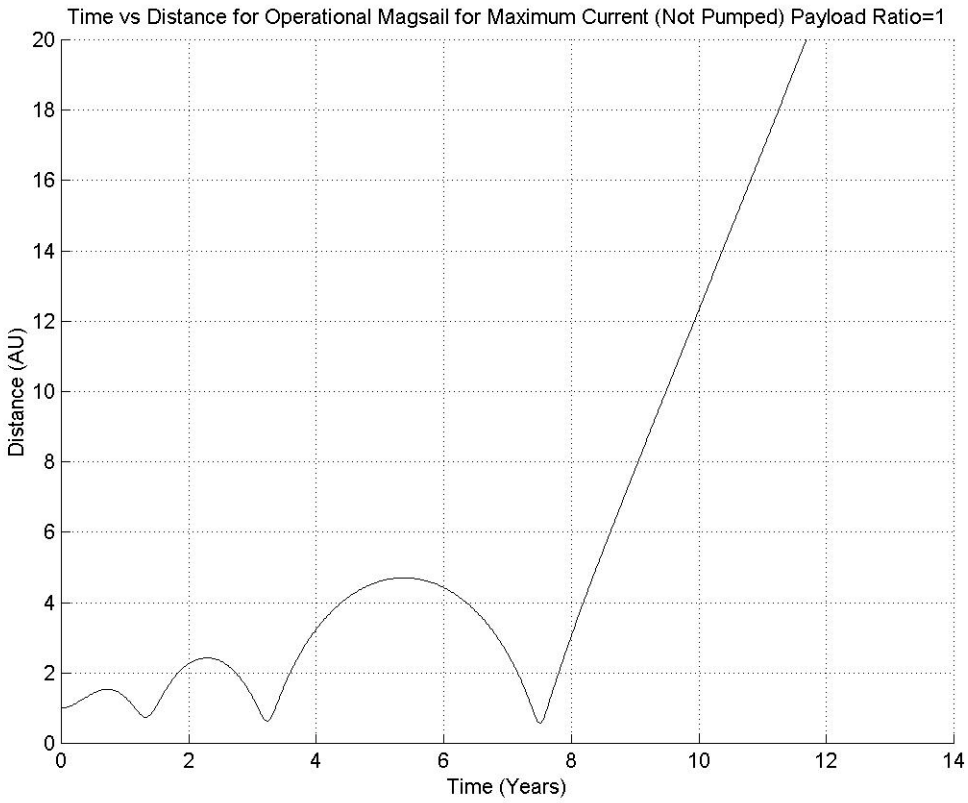

Fig 20: Time Vs. Distance for Maximum Current, Modified pumping, payload ratio=1 (Magsail turned off on Sunward orbit and also turned off at farther than 1.5 AU , until perihelion has decreased below 0.56 AU.)

The average speed vs. time for the previous four cases are compared in Fig. 24, showing maximum final speed of ~ 5 AU/yr. Such a spacecraft would take move into the vicinity of the Kuiper Belt, termination shock, and heliopause at ~ 100 AU in under 30 years.

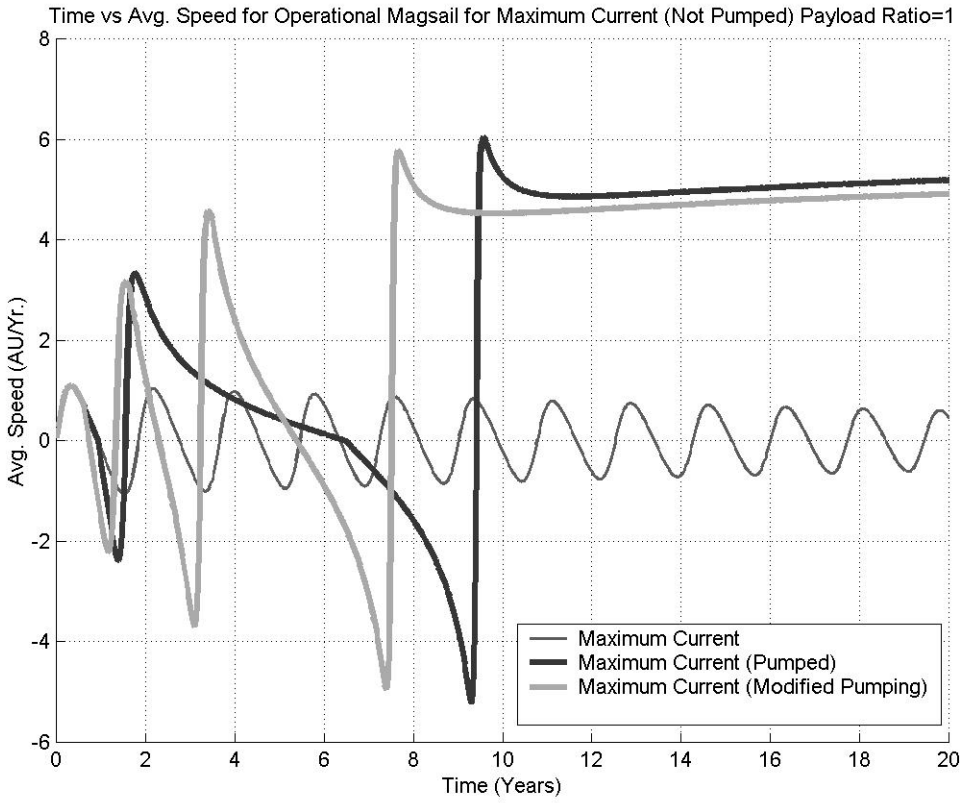

Fig 24: Time Vs. Average Speed for Previous Three cases of Maximum Current, payload ratio=1

Venus can be used to redirect the magsail, and make its mission more flexible. (Moving its orbit out-of-the-plane of the ecliptic could allow novel observations as well allow the higher speed solar winds to be utilized)

The lowest periapsis theoretically possible from an initial 1 AU Heliocentric orbit would be 0.50 AU. However, Mercury could still be reached be gravity assists or other means. At Mercury the hottest part of the MLI should only reach 491.6 K well below Kapton's upper temperature limit ~ 670 K -- which would be reached at 0.208 AU.

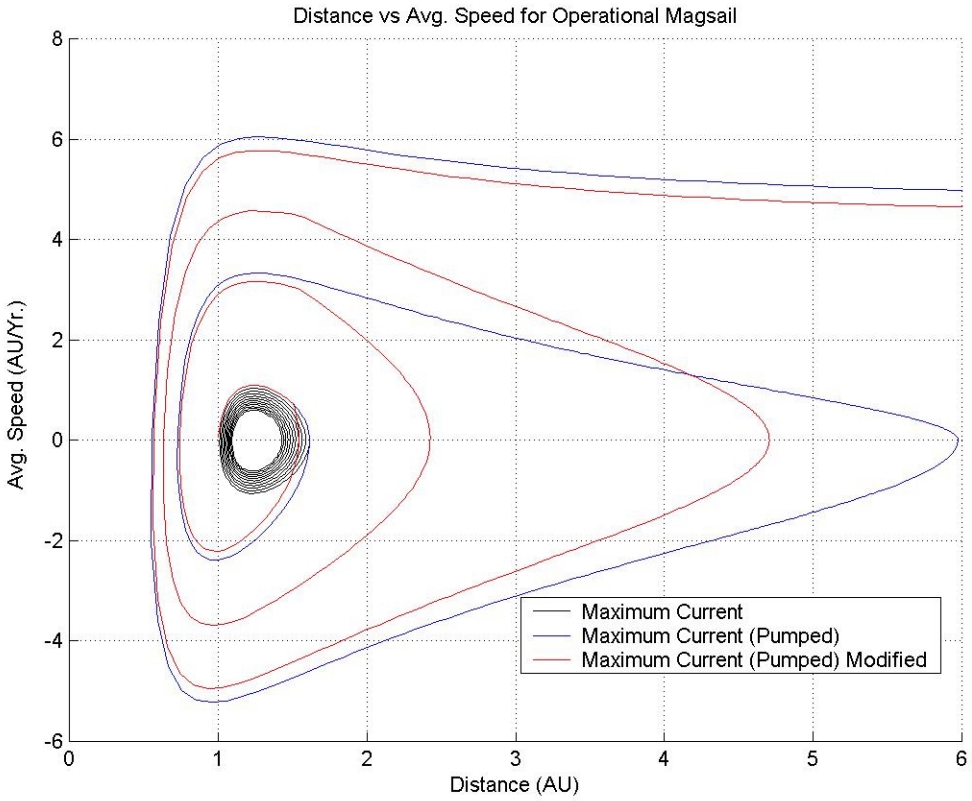

Fig 22: Distance Vs. Average Speed for Previous Three cases of Maximum Current, payload ratio=1

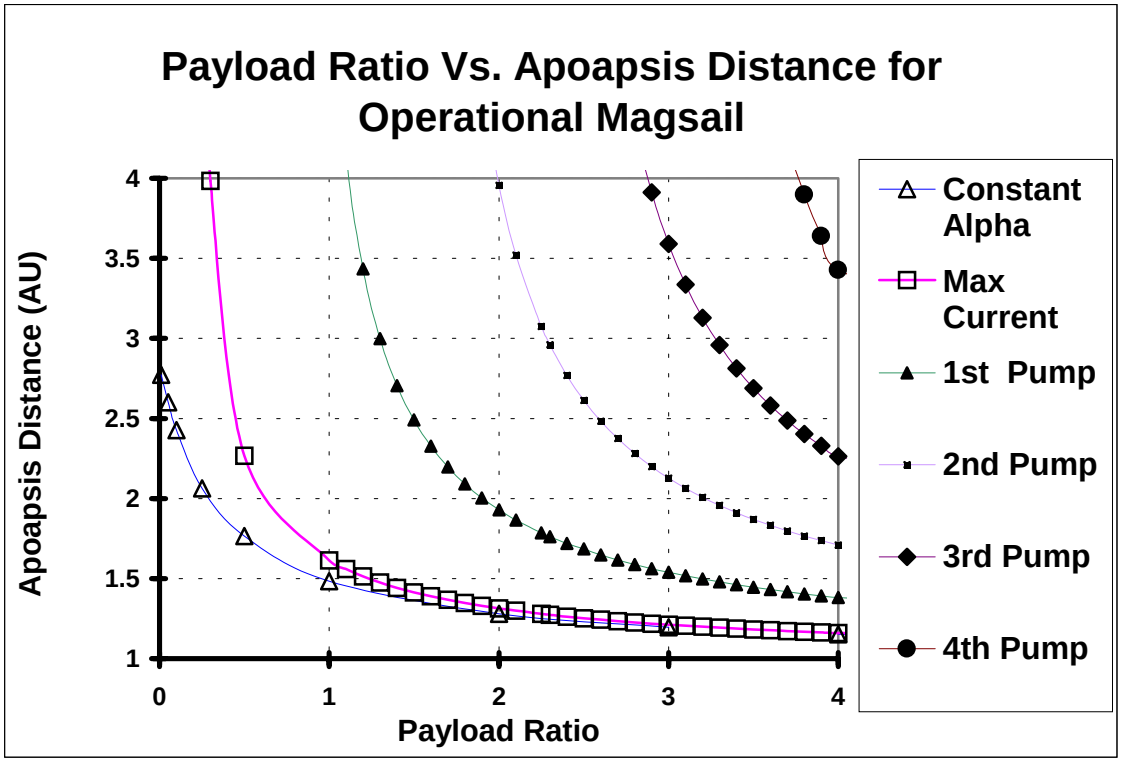

Fig 23: Payload Ratio vs. Apoapsis Distance for Operational Magsail, (pumped vs non-pumped)

A comparison of the constant alpha, maximum current, and pumped orbit modes for the operational magsail is shown in Fig. 23.

It can be seen that for payload ratios (payload mass/unloaded magsail S/C mass) of 0.5, the constant alpha orbit allows an apoapsis of 1.7 AU to be reached, while the Maximum current mode allows the spacecraft to reach about 2.3 AU. This is a significant improvement. However it can also be seen that for payload ratios greater than 1, the advantage of the Maximum current mode over the constant alpha mode becomes marginal.

But if pumping is used, a much more dramatic improvement is seen. The constant alpha spacecraft can reach 1.5 AU (Mars) with a payload ratio of about 1.0, the maximum current spacecraft can reach this same apoapsis with a payload ratio of about 1.2. But if orbit pumping is employed, the spacecraft can have its cargo tripled (payload ratio of 3). In that case, it would reach only about 1.25 AU on its first orbit, but then reach Mars on the second orbit with three times the cargo otherwise possible. To reach Ceres, at 2.7 AU, the constant alpha spacecraft could only have a payload ratio of about 0.1, the maximum current spacecraft could have a payload ratio of around 0.4, but a spacecraft employing 1 pumping orbit could have its payload ratio increased to 1.4, if 2 pumping orbits are employed, the payload increases further to 2.4, and if 3 pumps are used, a payload ratio of 3.5 can be attained. Thus, by using pumping, in 3 orbits the payload capability of the

operational magsail can be multiplied 35 times over compared to one following a simple constant alpha trajectory!

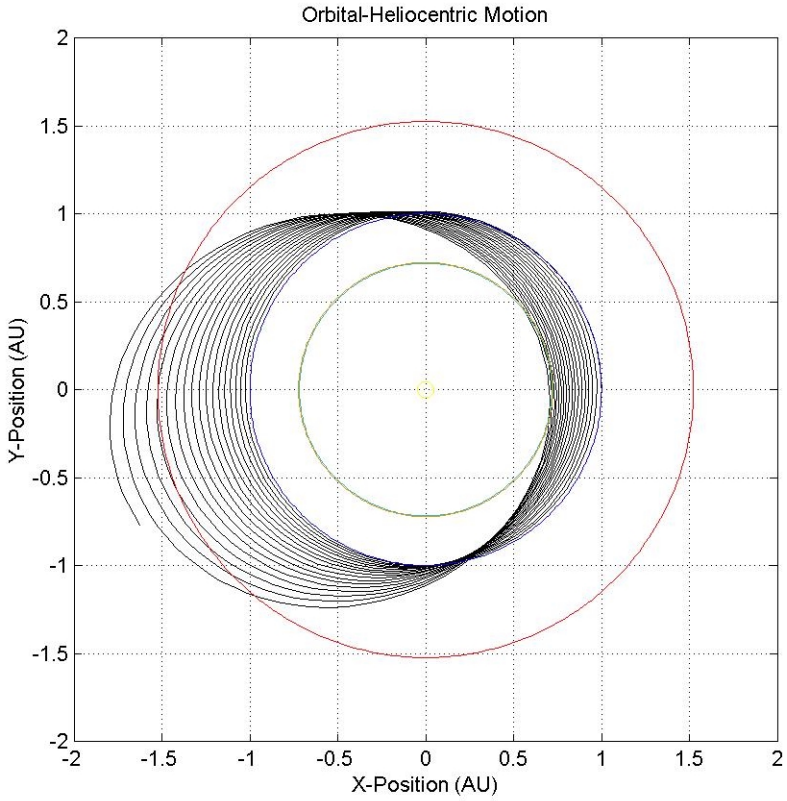

Fig 24: Orbit of Demonstrator Magsail
Orbits of Venus, Earth, and Mars also shown

As shown in Fig. 24 , orbit pumping can tested with the near-term demonstrator. With maximum current and pumping, the Demonstrator slowly raise its orbit to 1.0257 AU in 6 months, 1.11 AU in about 3.6 years and will reach Mars' orbit in 14.56 years. Its orbit will continue to increase until is escapes the solar system. (Fig 25)

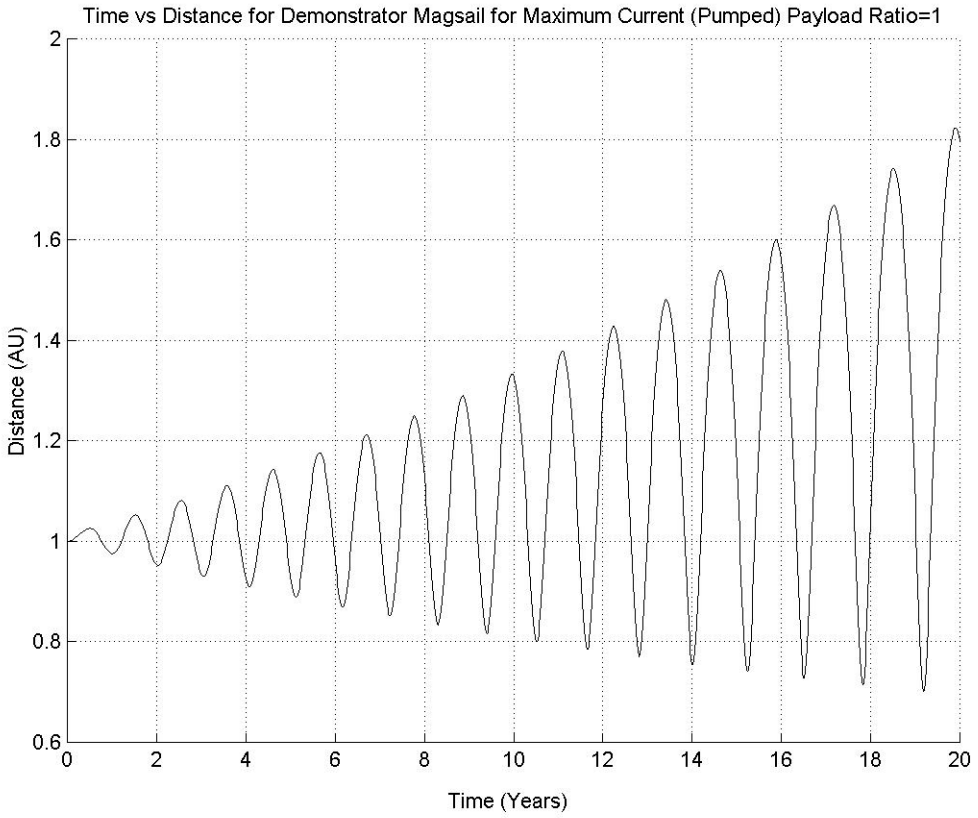

Fig 25: Time vs Distance for Demonstrator magsail

Operation in Solar Wind Environment:

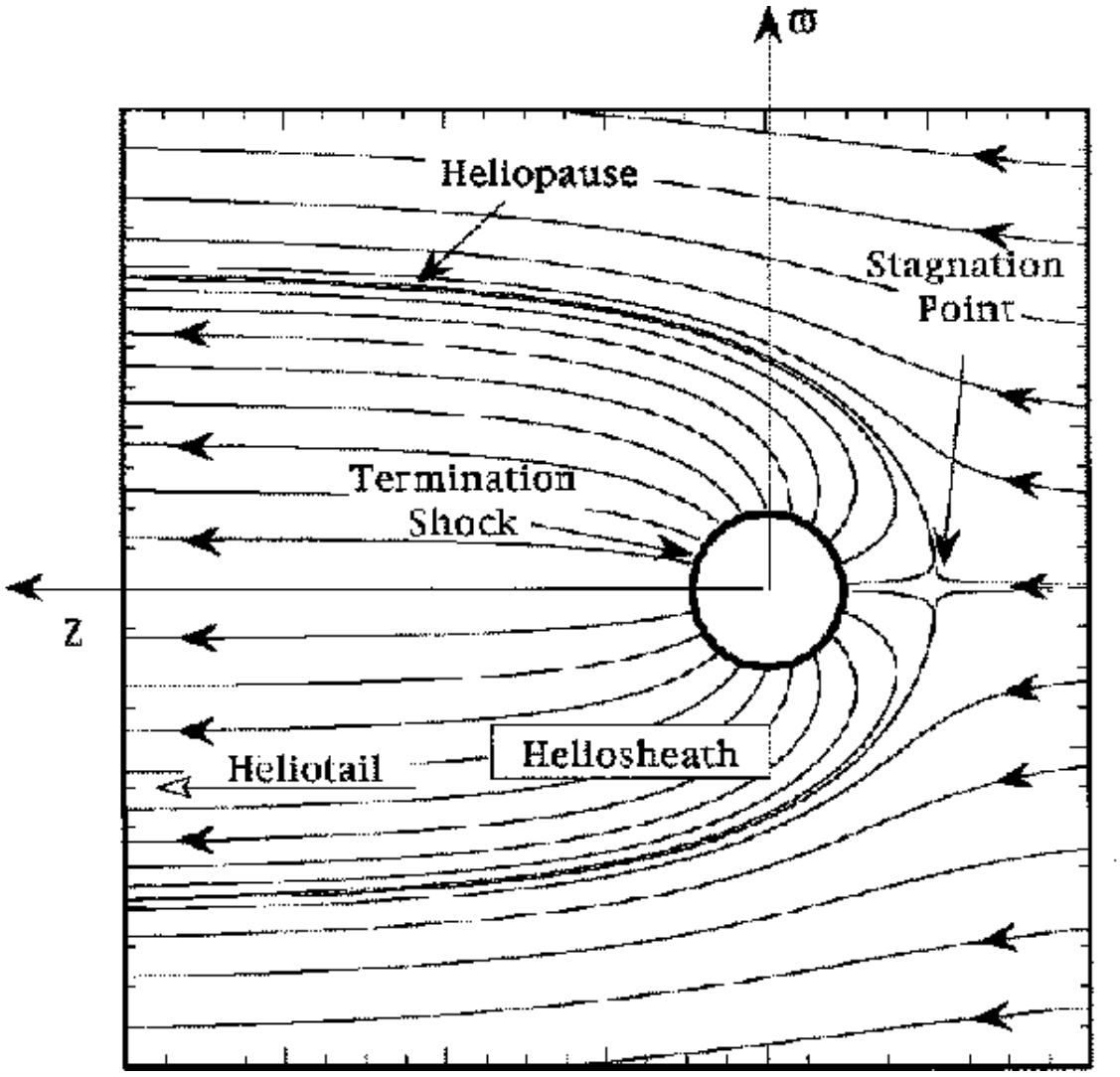

Fig 26: Streamlines in the Heliosphere: (Axford and Suess)[49]

The solar wind, which propels the magsail, blows a bubble in the local interstellar medium, called the heliosphere. Inside the hemisphere, the solar wind slows down to subsonic speeds at a certain distance, called the termination shock, where it piles up and slows to a stop, and slams into the interstellar medium at the edge of the heliosphere, the heliopause. Because the solar wind slows down at the termination shock, it is assumed that the magsail is turned off at this point. (Or very soon thereafter) See (Fig 26, Fig 27)

However the distance to the termination shock is not well know and varies from its minimum value near the solar apex (direction which the Sun is traveling towards) to a value over twice as large near the solar anapex (opposite direction). Estimates currently place the termination shock at 65-100 AU (with the higher values favored) and heliopause at 90-130 AU [49,50].

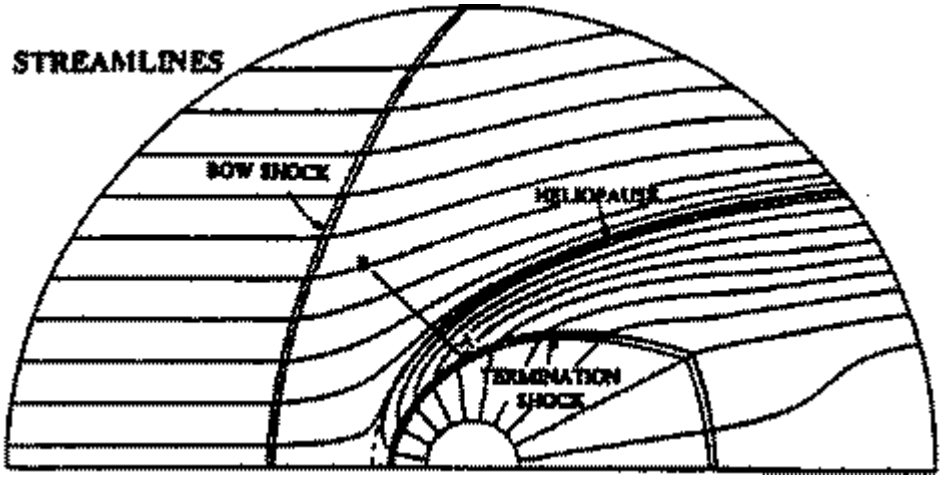

Fig 27: Streamlines in the Heliosphere: Closeup showing Termination Shock (Axford and Suess)[49]

Using these value for the termination shock, an advanced magsail with ten times the current density of the Operational magsail, normal orbit pumping, and a 0.05 payload ratio could reach 1,448 AU to 1,494 AU in 100 years flying through the nose of the termination shock (upstream), or over 1,519 AU to 1,555 AU flying through the tail of the termination shock (downstream).

Even at the lower size limits for the termination shock, a significant part of the shock would lie greater than 100 AU away. Flying to a 100 AU termination shock would allow speeds up to 15 AU/year to be obtained. Such a magsail could reach 1,000 AU in 67.2 yrs and 1,500 AU in 100 years. (Fig. 28)

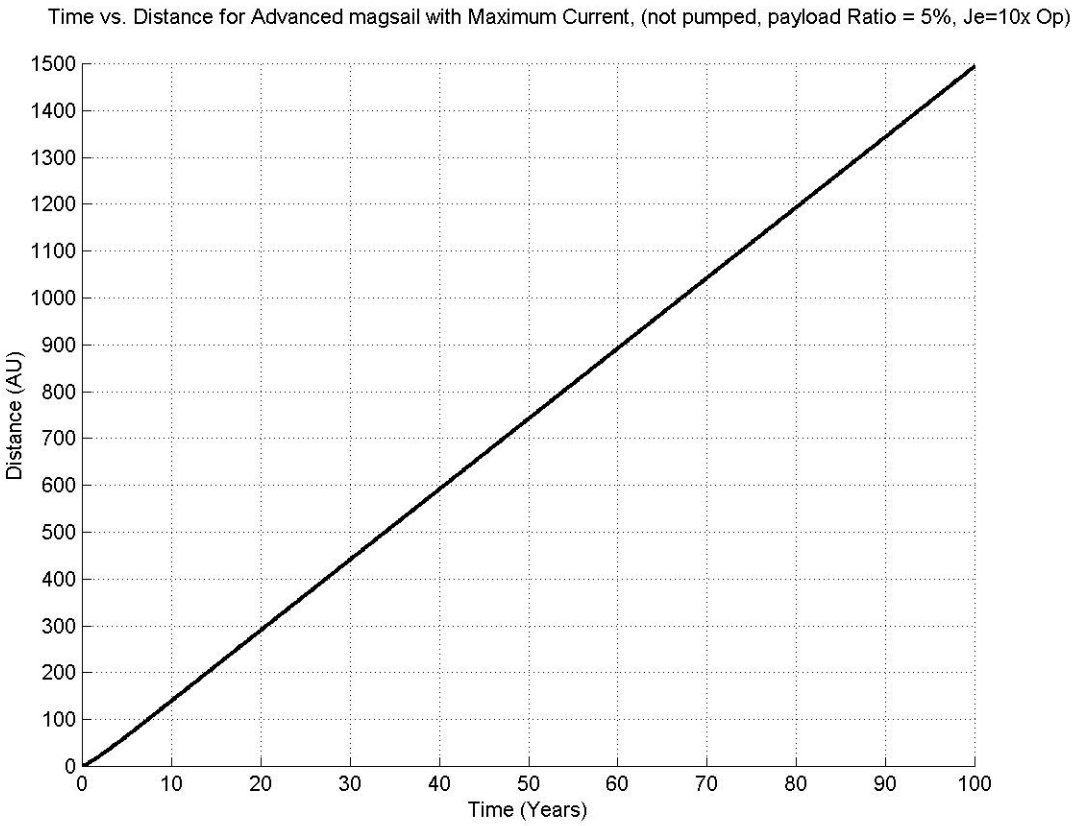

Fig 28: Time vs Distance for Advanced magsail with 10 times the current density of the Operational Magsail and 0.05 Payload Ratio, assuming a 100 AU Termination Shock

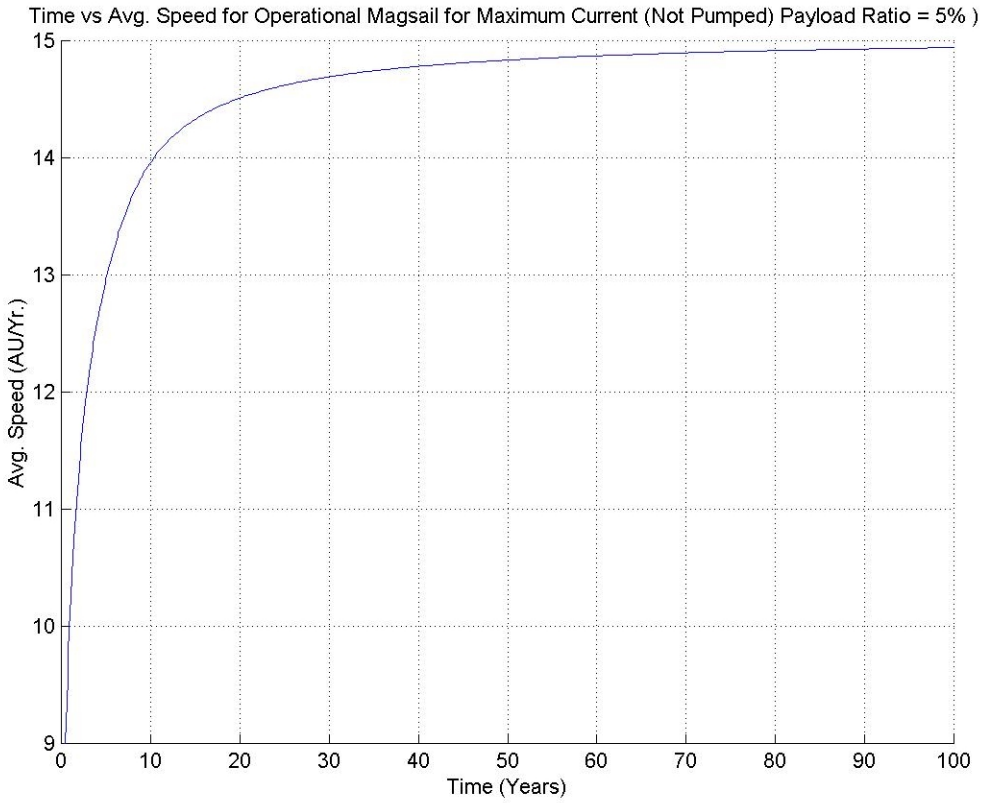

Fig 29: Time vs. Average Speed for an Advanced magsail with 10 times the current density of the Operational Magsail and 0.05 Payload Ratio, assuming a 100 AU Termination Shock

Normal Interaction with Solar Wind:

The nominal solar wind in assumed to change on the scale of months, as the Sun rotates, and years, for the sunspot cycle. The primary effects are expected to be transient periods of enhanced or decreased magsail thrust. This effect should not require active control other than normal attitude control. The effects on magsail performance are expected to smooth out over its flight time of several months/years.

In the ecliptic, the solar wind speed is assumed to range from a minimum of ~250 m/s to a maximum of ~ 800 m/s. A more typical range of 350 m/s to ~550 m/s can be seen in Fig 30 below from Voyager 2. The effective average of 480 m/s has been used in the more advanced orbit calculations. The speed of any particular parcel of solar wind is assumed to remain constant radially in space, from beyond a few solar radii to the termination shock. At the termination shock it rapidly slows down, which has not been analyzed here. Above the ecliptic there is a strong increase in solar wind speed. (see Figs.31, 32), which may be useful to boost magsail performance.

In the ecliptic, the density of the solar wind is assumed to average $8.35 \times 10^{-21}/R^2$ kg/m^3, where R is the distance of the spacecraft from the Sun in AU. Though the maximum solar wind density is about 1,000 times greater than its minimum value (Fig. 30,) such extremes are transient, and the variations are assumed to smooth out over time to the average values are used in calculations.

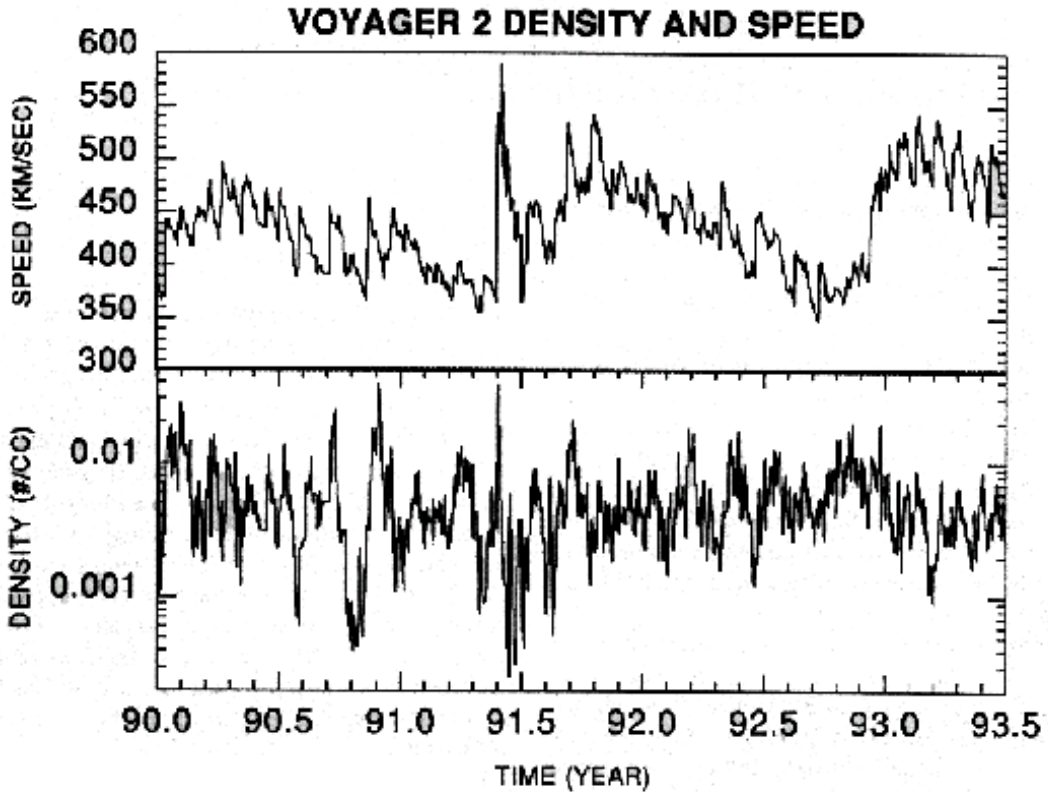

Fig 30: Voyager Solar Wind Density and Speed: One-day averages of the solar wind speed observed by Voyager 2 between January, 1990 and June, 1993 [Belcher et al., 1993] as cited by Neugebauer [51]

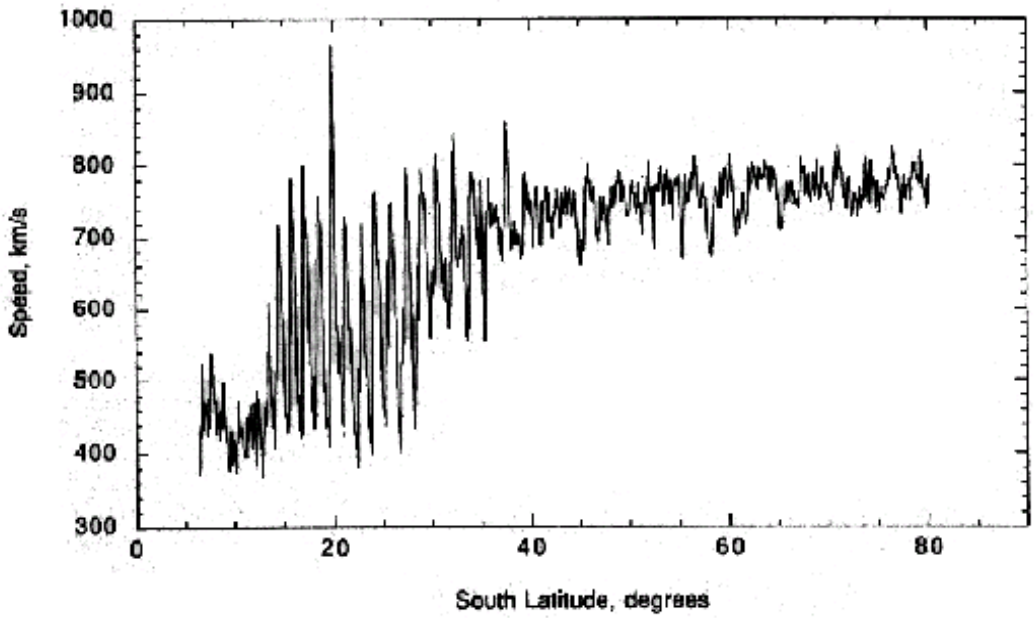

Fig 31: Solar Wind Average Speed vs. Heliograpic Latitude Twelve-hour averages of the solar wind speed observed by Ulysses versus heliographic latitude from February, 1992 through September, 1994 (after [Phillips et al., 1994]) as cited by Neugebauer [51]

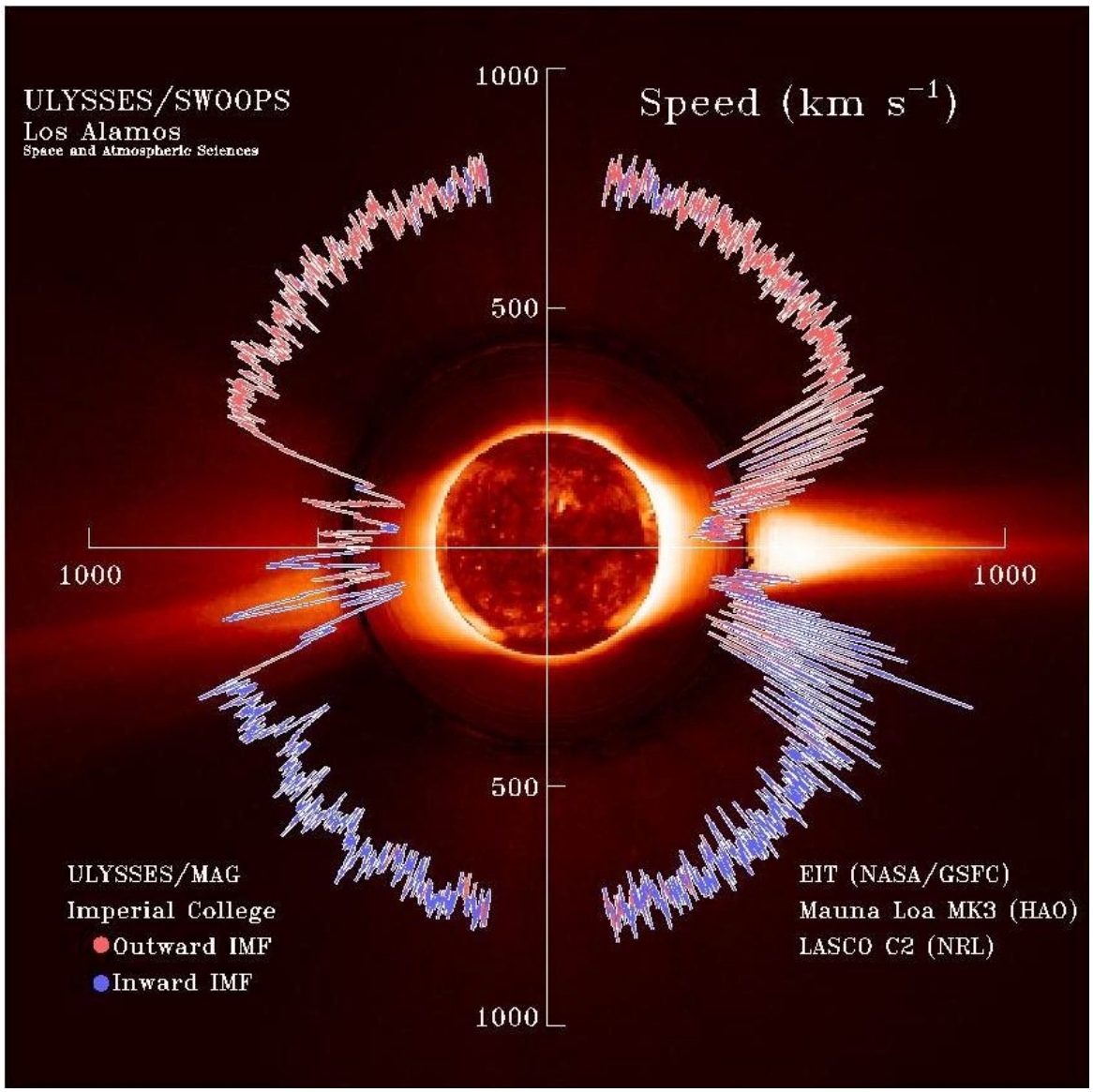

Fig 32: Solar Wind Average Speed vs. Heliograpic Latitude [52]

Interaction with Solar Flares:

The magnetosphere formed by the magsail will provide some shielding from solar radiation as it deflects charged low energy components of the solar wind (mainly protons). During periods of heightened solar activity, such as solar flares and coronal mass ejections, the mass and speed of the solar wind may increase dramatically. The bulk of the lower energy charged particles will be deflected by the magsail as long as the magnetosphere does not collapse, i.e., the magsail's magnetic field pressure in the center of the magsail, $B_m^2/2\mu$, remains above the plasma stream dynamic pressure of the solar

wind, $\rho_w V^2/2$.[14] (Where B_m = magnetic field at center of magsail, ρ_w = solar wind density and , V = solar wind velocity.)

Much data on solar wind variation exists from the Ulysses and Voyager spacecraft. The highest solar wind speed measured by Ulysses was 1,000 km/s near 20 degrees south heliographic latitude. (Fig 31, Fig 32) This is about twice the average value used in this study. At the ecliptic, the solar wind velocities observed by Voyager 2 (Jan. 1990 June 1993) did not reach above 600 km/s (see Fig 31), about 25 % above the assumed value.

Voyager 2 encountered two solar wind density spikes around 0.05 particles per cubic centimeter when the spacecraft was between 31-39 AU from the Sun. (Fig 30). (For comparison, these peak densities are about one-hundredth of the normal density value at 1 AU, but an order of magnitude larger than the normal values at 31 AU.) If the solar wind is assumed to be 100 % protons with its density decreasing as the inverse square of its distance, the solar wind density must have jumped to roughly 9.89 x 10^{-20} kg/m^2 at 1AU, in order to produce the values measured by Voyager 2. This 1 AU peak value is about 11.8 times the average value used in this study. At Venus this peak jumps to 22.6 times the average density used, and at Mercury about 79.0 times.

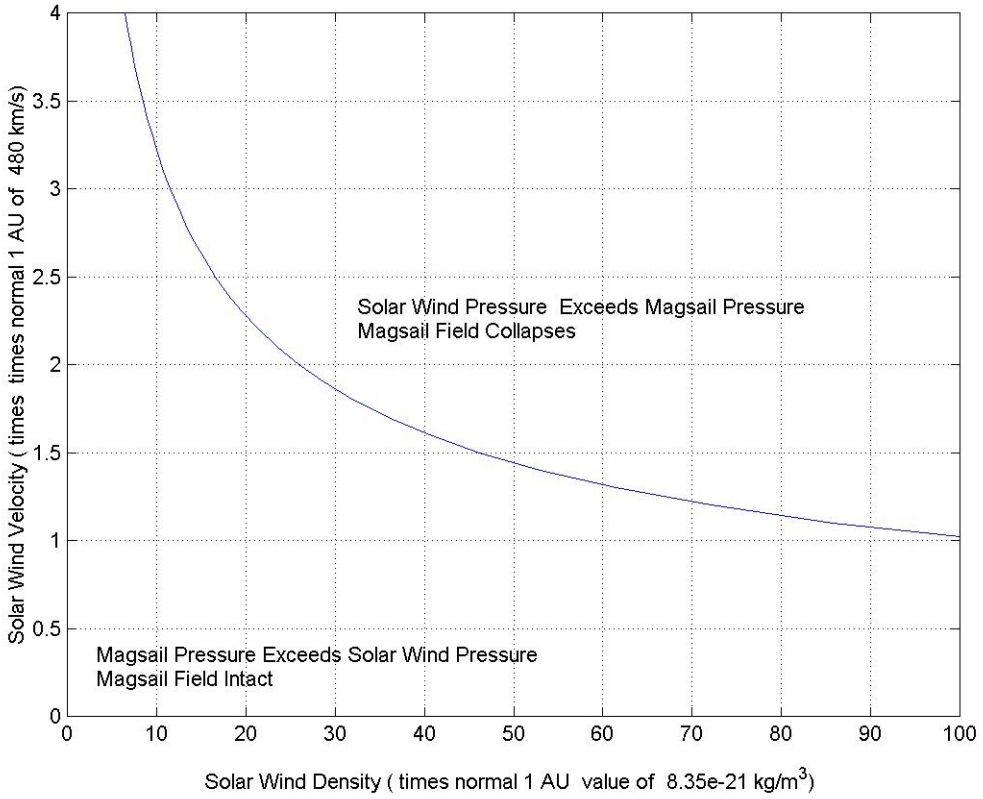

Fig 33. Solar Wind Pressure Compared with Magsail Magnetic Pressure, N/m^2 as a function of Solar Wind Speed and Density

From Fig 33 it is apparent that the operational magsail's field should stay intact for most foreseeable situations. The pressure of magsail's magnetic field will usually be stronger

than the pressure of the solar wind it is deflecting. The only times that the magsails' field should collapse will be during periods of strong solar activity when the magsail is very close to the Sun, near Mercury or closer, and/or at higher solar latitudes within Venus' orbit. (20 degrees latitude has been especially active in the past.) At those times, the higher pressure of the solar wind will cause the magsail's spherical magnetic field to collapse into a skinny toroidal field, which will only be strong enough to deflect a very small portion of the solar wind near the magsail's coil.

Transient Operation Near Sun:

As previously mentioned, the magsail's field could collapse very close to the sun, near Mercury or at higher solar latitudes. In addition, if the magsails travels much closer to the Sun than 0.208 AU, the temperature of outer surface of the MLI could rise above 400 C and the Kapton in the MLI may be damaged. If the magsail uses a higher Temperature MLI or stays farther out from the Sun, its MLI should remain undamaged and its interior temperature should not rise more than a few degrees above its 1AU temperature. In normal operations, starting from 1AU circular orbits, magsails will not be able to lower their periapsis below 0.50 AU before acquiring enough energy to escape the solar system, however extensive use of gravitational assists might be able to send a magsail inside Mercury's orbit at 0.39AU.

The Magsail as an Interstellar Brake.

While further in the future than interplanetary missions, one of the most important applications of magsails in the long term may be their utilization as braking systems for interstellar spacecraft accelerated to ultra-high velocities by other systems, such as fusion rockets or laser-pushed light sails. The magsail can accomplish such deceleration maneuvers without the use of propellant by creating drag against the interstellar medium. Assuming an operational temperature of 2.7 K, 10^5 kg of payload, and no insulation, a scaled-up version of the near-term Operational magsail with a 100 km radius , a wire density of 8 x 10^3 kg/m^3, an engineering current density of 10^9 A/m^2 at 77 K, a 15.3 mm thick wire, and a payload ratio of 0.0071, would take about 800 days to slow a spacecraft from 0.950 c to 0.582 c. Acceleration would start at 0.222 gee's and decrease to 0.116 gee's, neglecting relativistic effects and assuming a interstellar proton density of 10^5 protons/ m^3

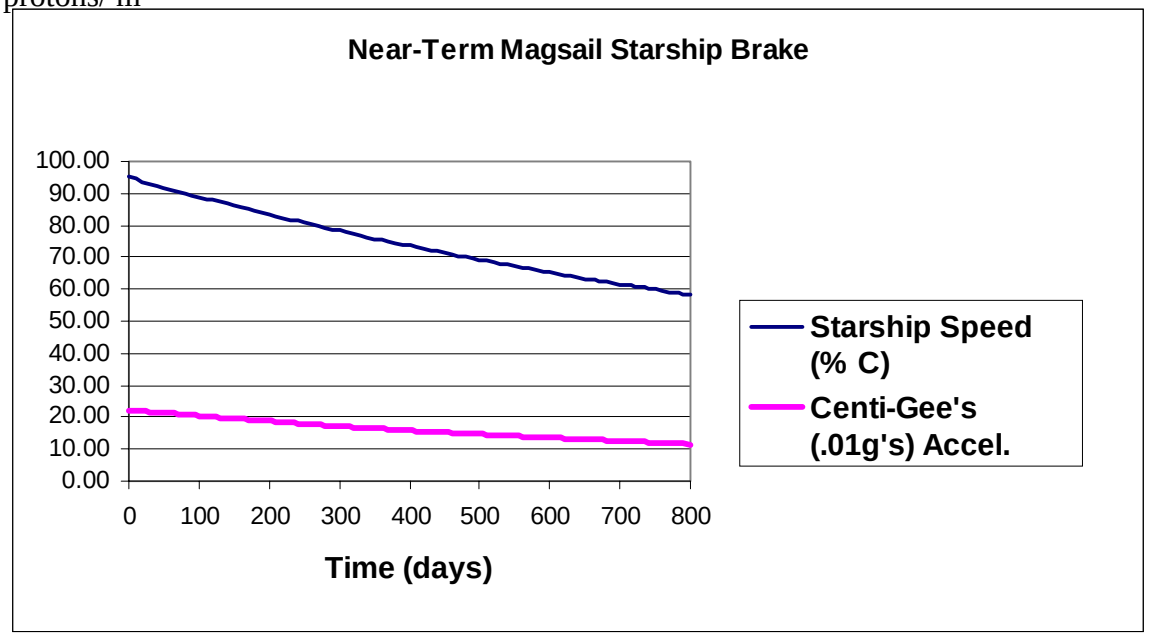

Fig. 34. Performance of the near-term operational Magsail as an interstellar brake.

However, the operational magsail is based on technology expected to be available within the next decade, so it may represent a much too conservative baseline for interstellar missions. It is therefore useful to consider a magsail based on YBCO researchers predictions for their technology several decades into the future. Such an advanced 100 km radius magsail, generating the same magnetic field, B_m= 1.0 x 10-6 T, (with a wire density of 7 X 10^3 kg/m^3, an engineering current density of 10^{11} A/m^2 at 77 K, a 1.53 mm thick wire, and a payload ratio of 0.8088) could decelerate a starship traveling at 95 % lightspeed to about 4 % lightspeed in ~320 days, 1% in ~ 620 days, and 0.56% in 800 days Deceleration would start at 5.47 g's but would later fall to 0.0058 gees.

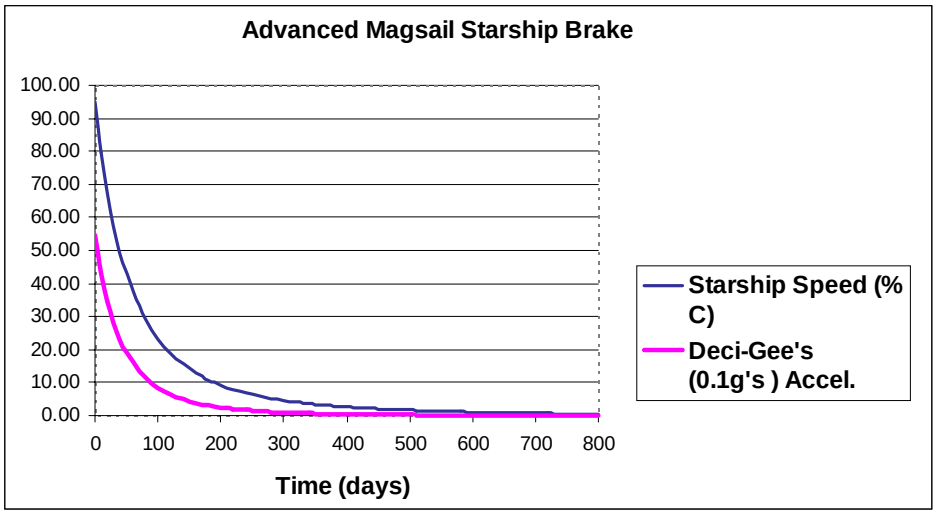

Fig. 35. Using an advanced magsail to decelerate a relativistic interstellar spacecraft.

By providing a means of decelerating a relativistic interstellar spacecraft within time scales of a year without the need for propellant, such advanced magsails may be an enabling technology for eventual human missions to the stars.

Proposed Magsail Experimental Program

The mathematics for calculating potential magsail performance has been worked in considerable detail, and a technology study has been conducted that indicates that the technology, design, and operability surrounding this very promising technique for space propulsion are all tractable. What is needed now to move magsail technology forward towards realization is some fundamental experimental work to validate the magsail performance equations and show that the key technological issue, deployment, uncovered in the course of the Phase I study is resolvable.

With this in mind, Pioneer Astronautics believes that an experimental Phase II investigation of magsail technology to move magsails rapidly from their current concept stage to flight demonstration is warranted. This follow-up program would include;

* Measurement of the mechanical properties of state of the art BSCCO derived magsail cable.
* Development of a simulation code using this data to allow magsail deployment using normal current electrodynamic forces to be simulated.
* Laboratory experiments to measure the lift and drag forces on a dipole in a plasma wind.
* Development of a magsail orbital flight experiment.

A proposal describing such a research program has been delivered by Pioneer Astronautics to NIAC for its consideration.

Conclusions

We find that high temperature superconducting cable should soon become with current densities sufficient to enable magnetic sail devices with the potential to move very large payloads from Earth orbit to anywhere in the solar system. Such magsails offer the advantage that they require no propellant, and can accomplish orbit transfer maneuvers without regard to the usual ballistic transfer launch windows. The required flight times for direct flights are slightly greater than the usual Hohmann transfer ballistic flight times. If pumping of orbits is employed, the payload delivered can be increased at will, albeit at the cost of increased transit time. Compared to a conventional solar lightsail, the magsail offers a thrust to weight ratio one to two orders of magnitude greater, as well as a system that is far more robust. The magsail also offers promise as an enabling technology for interstellar missions by providing a braking device which requires no propellant. A phase I examination of the technology and operational issues associated with magsails has indicated that they are all tractable, and that with effort, operational magsails could be made a reality in the relatively near future. Such systems could revolutionize our capabilities for the exploration and development of space.

We therefore recommend that the development of magsail technology be aggressively pursued

References

1) D.G. Andrews and R.M. Zubrin, "Magnetic Sails and Interstellar Travel," 39th Congress of the International Astronautical Federation, IAF-88-553, Bangelore India, Oct. 1988. Published in the Journal of the British Interplanetary Society, 1990.

2) R. M. Zubrin and D. G. Andrews, "Magnetic Sails and Interplanetary Travel," AIAA-89-2441, AIAA/ASME 25th Joint Propulsion Conference, Monterey, CA, July 1989. Published in Journal of Spacecraft and Rockets, April 1991.

3) D.G. Andrews and R.M. Zubrin, "Use of Magnetic Sails for Mars Exploration," AIAA-89-2861, AIAA/ASME 25th Joint Propulsion Conference, Monterey, CA. 1989.

4) D.G. Andrews and R.M. Zubrin, "Progress in Magnetic Sails," AIAA 90-2367, AIAA/ASME 26th Joint Propulsion Conference, Orlando, FL 1990.

5) G. Vulpetti, "Achievement of Rectilinear Trajectories in the Solar System by Non-Rocket Propulsion," IAF-90-303, 41st Congress of the International Astronautical Federation, Oct. 1990, Dresden, Germany.

6) G. Vulpetti, "The Two-Sail Propulsion Concept," IAA-91-721, 42nd Congress of the International Astronautical Federation, Oct. 1991, Montreal, Canada.

7) S.G. Love and D. G. Andrews, "Applications of Magnetic Sails," IAF 91-245, 42nd Congress of the International Astronautical Federation, Oct. 1991, Montreal, Canada.

8) R. Pool, "Good News for Superconductors," Science, p.755, Nov. 10, 1989.

9) J.R. Spreiter and A.Y. Alksne, "Plasma Flow Around the Magnetosphere," Proceedings of the International Symposium on the Physics of the Magnetosphere, Sept. 1968, Wash, D.C.

10) R.R. Bate, D.D. Mueller, and J.E. White, "Fundamentals of Astrodynamics," Dover Publications, New York, 1971.

11) A. Meinel and M. Meinel, "Thousand Astronomical Unit Mission," Presented to the National Commission on Space, August. 21, 1985.

12) K.T. Nock and A.L.Friedlander, "Elements of a Mars Transportation System," 37th Congress of the International Astronautical Federation,IAA-86-466, Innsbruck, Austria, Oct. 1986.

13) R. Zubrin, “The Use of Magnetic Sails to Escape from Low Earth Orbit,” Journal of the British Interplanetary Society, Vol. 46, pp.3-10, 1993.

14) Zubrin, Robert M., “The Use of Magnetic Sails to Escape From Low Earth Orbit”, Journal of the British Interplanetary Society, Vol. 46, pp. 3-10, 1993.

15) Shah, N., “Lunar Magsail: Conceptual Magnetic Sail Design for Lunar Missions”, 31st AIAA/ASME/SAE/ASEE Joint Propulsion Conference and Exhibit, July 10-12, 1995

16) Private communications with Lesh Motowidlo, IGC Advanced Superconductors, June 30, 1998

17) Lide, David R. (Editor-in-Chief), Handbook of Chemistry and Physics: 76 Edition, CRC Press, New York, 1995, p 12-173.

18) Larbalestier, David C., “The Road to Conductors of High Temperature Superconductors: 10 Years do make a difference!”, IEEE Trans. On Applied Superconductivity, Vol. 7, No.2, June 1997, (downloaded from http://www.engr.wisc.edu/centers/asc/pdfpapers.html)

19) Heussner, R.W., Nuues, C. Bormio, et al., “Properties of Niobium-Titanium Superconducting Wires With Nb Artificial Pinning Centers”, J. Appl. Phys. 80 (3), August 1,1996, (downloaded from http://www.engr.wisc.edu/centers/asc/pdfpapers.html)

20) Seeber, B., Handbook of Superconductivity, "Critical Current of Wires", Bernd Seeber (editor): Institute of Physics Publishing, Philadelphia,1998, p307-324,

21) Tenbrink, Johannes, Handbook of Applied Superconductivity, "General Aspects of High Temperature Superconductor wires and tapes", Bernd Seeber (editor): Institute of Physics Publishing, Philadelphia,1998, p446-465

22) Lide, David R. (Editor-in-Chief), Handbook of Chemistry and Physics: 76 Edition, CRC Press, New York, 1995, p 12-84.

23) National Renewable Energy Laboratory, “At the Frontiers of Science: Superconductivity and its Electric Power Applications”, DOE/GO-100098-434 (July 1998)

24)Malozemoff, A.P. et al.,“HTS Wire at Commercial Performance Levels”, http://www.amsuper.com/superconductivity/comwir~1.html (manuscript received for “Applied Superconductivity '98” on September 14, 1998)

25) Private communications with Dr. Larry Masur, American Superconductor, November 10, 1999

26) “STSI 1998 Annual Report: Section 2: Research Accomplishments and Plans”, http://www.stcs.uiuc.edu.edu/98annualreport/sec2

27) Cai, X.Y., Polyanskii, A, et al., “Current-limiting Mechanisms in Individual Filaments Extracted from Superconducting Tapes”, Nature, Vl. 932, 30 April, 1998., pp 906-909.

28) Private communications with Dr. Dean Peterson, Leader of Superconducting Technical Center, Los Alamos National Laboratory, June 22; July 6, 1999.

29) Oak Ridge National Laboratory, “High Temperature Superconductors”,http://www.ornl.gov/HTSC/htsc.html, (updated 19 March, 1999)

30) Department of Energy, “MCT Takes Major Step Toward Commercial-Scale Superconductors; Licenses Key Patents from Oak Ridge National Lab”, http://www.ornl.gov/HTSC/com%20scale%20rel.html (released April 16, 1998

31) Lubkin, Gloria B, "Power Applications of High Temperature Superconductors", Physics Today, March 1996, p48-51

32) Department of Energy, “Superconductivity Lab Highlights”, http://www.eren.doe.gov/superconductivity/htshighlights.html, October 1996.

33) Private communications with Alan Hermann, Professor of Physics, University of Colorado at Boulder, June 15,1999.

34) Cerulli, John, “State of the Art Technology for Large Power Applications: Current Programs and Future Expectations”, IEEE Power Engineering Society, Winter Meeting, February 1999, NY”, pp 1096-1100.

35) Private communications with Dr. Bob Hawsey, Oak Ridge National Laboratory.

36) Private communications with Paul Berdahl, Lawerence Berkeley Laboratory

37) Private communications with Dr. Richard Blaugher, National Renewable Energy Laboratory

38) Larson, Wiley J., Wertz, James R., "Space Mission Analysis and Design", Microcosm and Kluwer Academic Publishers, California, 1996, p 416-430, 403

39) Private communications with Mike Coyle, Vice President Swales Aerospace

40) Larson, Wiley J., Wertz, James R., "Space Mission Analysis and Design", Microcosm and Kluwer Academic Publishers, California, 1996, p 393, 403.

41) Deep Space Systems Technology Program: X2000, Advanced Radioisotope Power Source (ARPS), http://dsst/jpl.nasa.gov/DSST_ARPS.html

42) NASA Advanced Technology and Mission Studies,
http://www.hq.nasa.gov/office/oss/osstech/solar.htm (updated May 7, 1998)

43) Deep Space Systems Technology Program: X2000 First Delivery,
http://dsst/jpl.nasa.gov/DSST_1st.htm

44) Oman, Henry (editor-in-Chief), "News from the 32nd IECEC: Energy Conversion", IEEE AES Systems Magazine, p18-19, June 1998

45) Allied Signal, Technical Data sheet on Spectra Fiber (AS-PF-PS9B)

46) Private communications with Dr. Robert Hoyt, Tethers Unlimited, September 9, 1999.

47) Private communications with Dr. Larry Masur, American Superconductor, June 15, 1999

48) "PHA (Potentially Hazardous Asteroids) Orbital Elements",
http://neo.jpl.nasa.gov/neo/pha_elem.htm

49) Axford, Ian, and Steven Suess., "The Heliosphere-A Short Review".,
http://web.mit.edu/space/www/voyager/voyager_science/helio.review/axford.suess.html

50) MIT Space Plasma Group, "The Voyager Interstellar Mission",
http://web.mit.edu/space/www/voyager_science.html

51) Neugebauer., M.,"Charting the Heliosphere in Three Dimensions"
http://earth.agu/revgeophys/neugeb01/node5.html

52) "MSFC Solar Physics: The Solar Wind",
http://wwwssl.msfc.nasa.gov/ssl/pad/solar/sun_wind.htm